NAVAL POSTGRADUATE SCHOOL

MONTEREY, CALIFORNIA

THESIS

SWEPT-RAMP DETONATION INITIATION PERFORMANCE IN A HIGH-PRESSURE PULSE DETONATION COMBUSTOR

by

Daniel A. Nichols

December 2010

Thesis Advisor:	Christopher M. Brophy
Second Reader:	Anthony J. Gannon

THIS PAGE INTENTIONALLY LEFT BLANK

REPORT DOCUMENTATION PAGE			Form Approved OMB No. 0704-0188
Public reporting burden for this collection of information is estimated to average 1 hour per response, including the time for reviewing instruction, searching existing data sources, gathering and maintaining the data needed, and completing and reviewing the collection of information. Send comments regarding this burden estimate or any other aspect of this collection of information, including suggestions for reducing this burden, to Washington headquarters Services, Directorate for Information Operations and Reports, 1215 Jefferson Davis Highway, Suite 1204, Arlington, VA 22202-4302, and to the Office of Management and Budget, Paperwork Reduction Project (0704-0188) Washington DC 20503.			
1. AGENCY USE ONLY ***(Leave blank)***	**2. REPORT DATE** December 2010	**3. REPORT TYPE AND DATES COVERED** Master's Thesis	
4. TITLE AND SUBTITLE Swept-Ramp Detonation Initiation Performance in a High-Pressure Pulse Detonation Combustor			**5. FUNDING NUMBERS** **N0001410WX20832**
6. AUTHOR(S) Daniel A. Nichols			
7. PERFORMING ORGANIZATION NAME(S) AND ADDRESS(ES) Naval Postgraduate School Monterey, CA 93943-5000			**8. PERFORMING ORGANIZATION REPORT NUMBER**
9. SPONSORING /MONITORING AGENCY NAME(S) AND ADDRESS(ES) N/A			**10. SPONSORING/MONITORING AGENCY REPORT NUMBER**
11. SUPPLEMENTARY NOTES The views expressed in this thesis are those of the author and do not reflect the official policy or position of the Department of Defense or the U.S. Government. IRB Protocol number _____N/A_____.			
12a. DISTRIBUTION / AVAILABILITY STATEMENT Approved for public release; distribution is unlimited			**12b. DISTRIBUTION CODE**

13. ABSTRACT (maximum 200 words)

Pulse detonation combustion technologies promise the potential of increased thermodynamic efficiency and performance, across a wide range of thrust and power generation applications. Thrust applications would require initial combustor pressures of about 1–4 atm while power applications would require about 4–20 atm. Most of the previous testing of Pulse Detonation Combustors (PDCs) utilized standard atmospheric pressure conditions at sea level, but at elevated temperatures of 300–500°F in the combustor. The current work was motivated by a need to experimentally evaluate the detonation initiation performance of a PDC at elevated combustor pressures. Detonability was evaluated at initial combustor pressures from 2–5 atmospheres and at equivalence ratios of about 0.9–1.1. The experimentation utilized a previously constructed and evaluated three inch diameter combustor that employed swept-ramps as the mechanism for Deflagration-to-Detonation (DDT) initiation. Ramps were removed as the pressure was increased to determine how many sets were necessary to achieve DDT. The legacy PDC was adapted with new and modified components, enabling it to operate at higher pressures and temperatures and for longer durations. It was found that for initial combustor pressures up to 5 atm at least four sets of ramps are required to achieve DDT.

14. SUBJECT TERMS Pulse Detonation Engine, PDE, Pulse Detonation Combustor, PDC, High-Pressure Combustor, deflagration-to-detonation, DDT, Swept-ramp			**15. NUMBER OF PAGES** 87
			16. PRICE CODE
17. SECURITY CLASSIFICATION OF REPORT Unclassified	**18. SECURITY CLASSIFICATION OF THIS PAGE** Unclassified	**19. SECURITY CLASSIFICATION OF ABSTRACT** Unclassified	**20. LIMITATION OF ABSTRACT** UU

NSN 7540-01-280-5500 Standard Form 298 (Rev. 2-89)
Prescribed by ANSI Std. 239-18

THIS PAGE INTENTIONALLY LEFT BLANK

Approved for public release; distribution is unlimited

SWEPT-RAMP DETONATION INITIATION PERFORMANCE IN A HIGH-PRESSURE PULSE DETONATION COMBUSTOR

Daniel A. Nichols
Lieutenant Commander, United States Navy
B.S., West Virginia University, 1997

Submitted in partial fulfillment of the
requirements for the degree of

MASTER OF SCIENCE IN ASTRONAUTICAL ENGINEERING

from the

NAVAL POSTGRADUATE SCHOOL
December 2010

Author: Daniel A. Nichols

Approved by: Christopher M. Brophy
Thesis Advisor

Anthony J. Gannon
Second Reader

Knox T. Millsaps
Chairman, Department of Mechanical and Aerospace Engineering

THIS PAGE INTENTIONALLY LEFT BLANK

ABSTRACT

Pulse detonation combustion technologies promise the potential of increased thermodynamic efficiency and performance, across a wide range of thrust and power generation applications. Thrust applications would require initial combustor pressures of about 1–4 atm while power applications would require about 4–20 atm. Most of the previous testing of Pulse Detonation Combustors (PDCs) utilized standard atmospheric pressure conditions at sea level, but at elevated temperatures of 300–500°F in the combustor. The current work was motivated by a need to experimentally evaluate the detonation initiation performance of a PDC at elevated combustor pressures. Detonability was evaluated at initial combustor pressures from 2–5 atmospheres and at equivalency ratios of about 0.9–1.1. The experimentation utilized a previously constructed and evaluated three inch diameter combustor that employed swept-ramps as the mechanism for Deflagration-to-Detonation (DDT) initiation. Ramps were removed as the pressure was increased to determine how many sets were necessary to achieve DDT. The legacy PDC was adapted with new and modified components, enabling it to operate at higher pressures and temperatures and for longer durations. It was found that for initial combustor pressures up to 5 atm at least four sets of ramps are required to achieve DDT.

THIS PAGE INTENTIONALLY LEFT BLANK

TABLE OF CONTENTS

LIST OF FIGURES

LIST OF TABLES

THIS PAGE INTENTIONALLY LEFT BLANK

LIST OF ACRONYMS AND ABBREVIATIONS

atm		atmosphere
C-J	-	Chapman-Jouguet
CCD	-	Charge-Coupled Device
DDT	-	Deflagration-To-Detonation Transition
NI	-	National Instruments
NPS	-	Naval Postgraduate School
PDC	-	Pulse Detonation Combustor
PDE	-	Pulse Detonation Engine
RPL	-	Rocket Propulsion Laboratory
STP		Standard Temperature and Pressure
VI	-	Virtual Instrument
VIS	-	Variable Ignition System
A	-	Area
C	-	carbon
C_2H_4	-	ethylene
c	-	speed of sound
C_P	-	constant pressure coefficient of specific heat
cm	-	centimeter
f	-	fuel-to-air ratio
GB	-	gigabyte
GHz	-	gigahertz
g	-	gravitational constant
H	-	hydrogen
Hz		hertz
K	-	Kelvin
kg	-	kilogram
MHz	-	megahertz
m	-	meter
mm	-	millimeter
m/s		meter per second

M	-	Mach number
MU		measurement unit
$\dot{m}$	-	mass flow rate
$\dot{m}_f$	-	mass flow rate of fuel
$\dot{m}_a$	-	mass flow rate of air
$\dot{m}_{tot}$	-	total mass flow rate
N	-	nitrogen
O	-	oxygen
p	-	pressure
pC		picocoulombs
psi	-	pounds per square inch
psig	-	pounds per square inch gage
P-v	-	pressure-specific volume
q	-	specific heat
R	-	specific gas constant
s	-	second
s	-	entropy
t	-	time
T	-	temperature
u	-	velocity
V_{det}	-	Detonation Velocity
v	-	velocity
φ	-	equivalence ratio
γ	-	specific heat ratio
ρ	-	density

ACKNOWLEDGMENTS

I would like to express my sincere gratitude to Dr. Christopher Brophy for his guidance, patience, and instruction throughout the development and completion of this thesis. His dedication to research and the mentorship of students was admired, and was invaluable in ensuring that this thesis was able to be completed on time and to provide an exceptional learning opportunity.

I would also like to thank Mr. George Hageman for sharing his extensive mechanical knowledge and his collection of humorous anecdotes, a balance which helped to make this process both educational and fun.

A debt of appreciation is also owed to Thomas Lipoma and Ashley Hobson, for their digital modeling in Solid Works and to Bobby Wright and Dave Dausen for sharing their technical knowledge and assistance.

Finally, I would like to thank my wife Julie, my daughter Zoey, and my son Evan, for their endless encouragement and support during this demanding time.

THIS PAGE INTENTIONALLY LEFT BLANK

I. INTRODUCTION

The development of Pulse Detonation Engines (PDE) has made many achievements in the past twenty-five years, yet the interest and development of this unique propulsion system started well before then. One of the earliest studies involving the use of intermittent detonations for propulsion was performed by Nichols et al. [1], in 1957, when experimental analysis predicted that high frequency detonations could produce significant thrust with a specific impulse exceeding 2,000 seconds. At the same time however, the performance of conventional Brayton cycle propulsion systems, such as turbo-jets and rockets, were rapidly improving. Thus, little interest was shown in the utilization of transient detonations for propulsive purposes which were much more dynamic, and more difficult to achieve reliably. In recent years, conventional propulsion systems have shown that they will not likely produce significant gains in technology or performance due to limitations in cycle efficiencies. PDEs promise increased thermodynamic efficiency and performance across a wider range of flight regimes.

While precise performance values vary in the literature, Figure 1 presents the performance of various propulsion concepts in terms of their relative specific impulse and Mach number regimes. A recent study did find that the specific impulse of a PDE is in the range of 36% higher than a ramjet at Mach 1.5, to 4% greater at Mach 5 [2]. Turbojets do offer an appreciably superior impulse at subsonic and low supersonic flight velocities, but they are costly and structurally and thermodynamically limited to about Mach 3–4 due to the compressor discharge conditions at high flight velocities. Ramjets and scramjets are capable of speeds well above Mach 4, but have a limited throttling capability and require a booster to accelerate them to operational velocities, resulting in a decrease in overall system performance and an increase in complexity. The PDE is envisioned as a possible alternative for the ramjet as it offers the advantages of high performance and efficiency across a broad range of speed regimes, in combination with a relatively simplistic design.

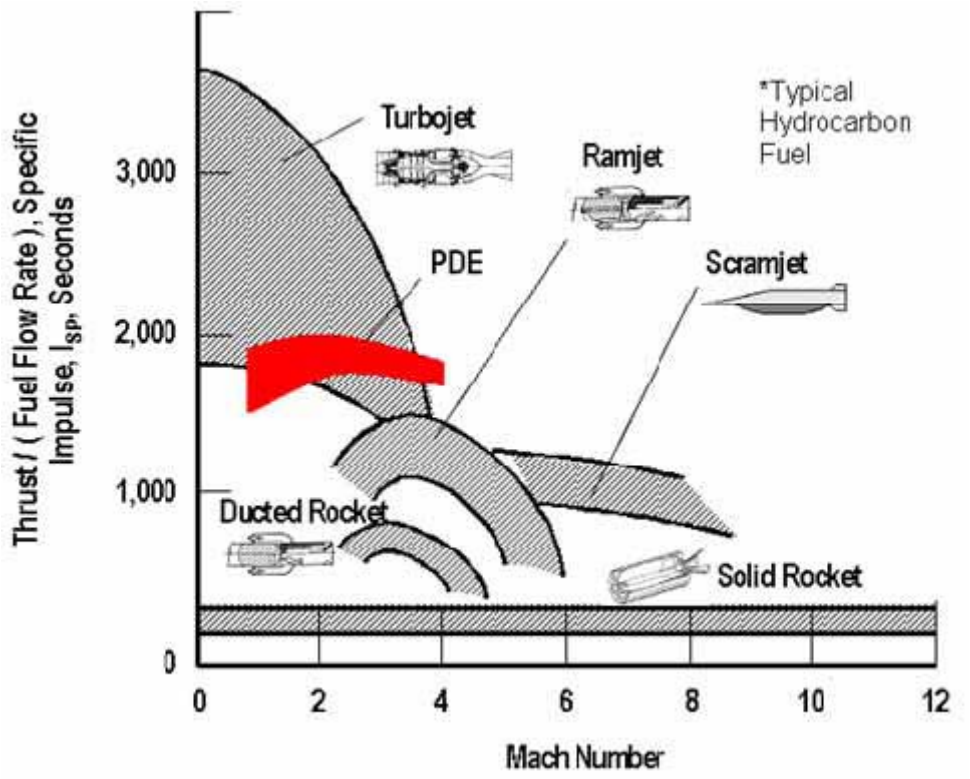

Figure 1. Comparison of High-Speed Propulsion Technologies (After [3])

PDEs are air-breathing propulsion systems that operate by initiating repetitive detonations in a combustion chamber filled with a fuel-air mixture. The combustor typically has an inlet, a nozzle at the exit, and is operated in a cyclical manner, multiple times per second. Without any moving machinery, the detonation wave generates significant chamber pressures, producing thrust by expanding the combustion products at the aft end of the combustor [4]. Near constant thrust is produced by repeating the process at a high frequency. Because the detonation event approximates a near constant volume combustion process, it has a much greater thermodynamic efficiency than conventional systems which operate under a constant pressure combustion process. This efficiency in combination with its simple design, make PDEs an attractive solution for many propulsion applications.

Based on our current understanding, the application of pulse detonation combustion could be applied as a propulsion system for missile systems, as a PDE, or for power generation applications, such as those used onboard a sea going vessel. One of the factors in the practical implementation of PDEs is the ability of the engine to operate at practical combustor conditions and with practical fuels. Most of the current testing of Pulse Detonation Combustors (PDCs) has been performed at a pressure of one atmosphere but at elevated temperatures (350–500°F). In reality, if a PDC where to be used for one of the previously mentioned applications the combustor would be exposed to higher pressure and temperature reactants prior to ignition.

Propulsion applications would likely require initial combustor pressures from 1–4 atmospheres (atm) while power applications would require initial combustor pressures from about 4–20 atm. It has been shown that as the initial pressure and temperature of the mixture increases the cell size of the combustion event decreases, and reflects the increase in the sensitivity of the mixture to undergo detonations [5].

The current work utilized portions of a previously constructed and evaluated PDC that included new components and some other slight modifications, enabling it to operate at higher pressures and temperatures and for longer durations. The combustor section and the nozzle were completely redesigned to include cooling jackets, allowing them to withstand the elevated temperatures over longer test durations. This also involved the design of a new cooling system. New fuel injectors with a greater mass flow rate replaced previous injectors as the pressure was increased and modifications were made to the fuel delivery system enabling longer duration operation. The PDC used existing swept-ramp obstacles from previous research for deflagration-to-detonation transition [6].

The goal of the study was to evaluate the detonation initiation performance of the PDC at high (2–5 atm) combustor pressures, and to determine the number of ramps necessary to achieve DDT at these associated pressures.

THIS PAGE INTENTIONALLY LEFT BLANK

II. BACKGROUND

A. COMBUSTION PROCESSES

1. General

To fully understand the pulse detonation engine cycle it is necessary to understand the difference between a detonation and the more common form of combustion, deflagration. Combustion occurs when fuel and oxidizers are combined and ignited, resulting in the rapid oxidation of the fuel. The result is a combustion wave that propagates away from the ignition source, producing a change in the mixture composition and an increase in enthalpy. The following sections discuss these two modes of combustion, highlight their differences, and introduce several concepts, which aid in the understanding of the detonation phenomenon.

2. Deflagration

A deflagration is a nearly constant-pressure combustion wave that propagates at subsonic velocities into unburned reactants. As the wave propagates through a reactive mixture, the combustion and resulting energy release occur only at the flame front. Combustion products are left behind the front without an increase in pressure and the release of energy provides a temperature increase to the fluid. The initial temperature and pressure of the reactants also affect the rate at which they are consumed. Finally, since the combustion can only occur when the flame front comes in contact with the reactants through the diffusion process, the local reaction rates limit the flame speed and hence ensure that the velocities remain subsonic. One primary characteristic of a deflagration is its constant-pressure nature, which results in a relatively large increase in entropy, resulting in lower thermodynamic efficiencies [7].

Examples of deflagrations are as simple as an open flame, to the more complex cases of the combustion of a fuel-air mixture in a gas turbine engine or a conventional rocket engine.

3. Detonation

Detonation is a combustion wave that propagates at supersonic velocities into unburned reactants and in the process significantly compresses the mixture. This compression results in an increase in pressure, temperature, and density until a violent exothermic reaction front further strengthens the leading shockwave. The interaction of the shockwave and combustion waves is self-sustaining as long as a combustible mixture is downstream of the detonation. Although a detonation releases almost the same amount of energy as a deflagration, it does so at a dramatically faster rate and with a lower increase in entropy and thus provides a greater work potential.

4. Comparison of Deflagration and Detonation

A comparison of the characteristics of deflagration and detonation waves is necessary to appreciate the differences between these two types of combustion. A one-dimensional model of a combustion wave in an infinitely long duct of constant cross-sectional area is given in Figure 2. The stationary combustion wave has unburned reactants moving towards the combustion wave with velocity u_1 and burned products moving away from the wave with velocity u_2.

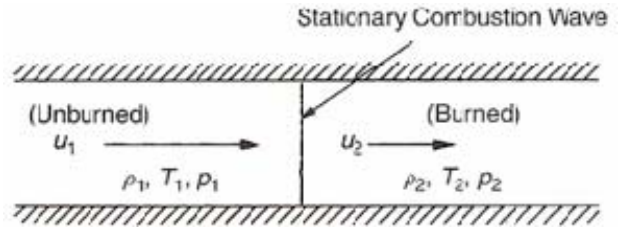

Figure 2. Stationary One-Dimensional Combustion Wave Model (From [7])

The ratios of the product properties to the reactant properties vary dependent upon whether the planar wave is representing a deflagration or a detonation wave. Typical values of the ratios of the critical velocities ($u_{1,2}$), densities ($\rho_{1,2}$), temperatures ($T_{1,2}$), and pressures ($p_{1,2}$) with respect to Figure 1 are given in Table 1 for both types of waves. The most notable differences are between the pressure and temperature ratios. A detonation

cycle results in a greater increase in temperature and pressure than deflagration. The resulting higher enthalpies for a similar heat release make detonation a much more efficient type of combustion.

	Detonation	**Deflagration**
u_1/c_1	5-10	0.0001-0.03
u_2/u_1	0.4-0.7 (deceleration)	4-16
p_2/p_1	13-55 (compression)	0.98-0.976 (slight expansion)
T_2/T_1	8-21 (heat addition)	4-16 (heat addition)
ρ_2/ρ_1	1.4-2.6	0.06-0.25

Table 1. Typical Characteristics of Detonation and Deflagration (From [7])

B. DETONATION THEORY

The post-combustion state thermodynamic properties and in turn the combustion process of detonation can be described further through the use of a Hugoniot curve in conjunction with the Rayleigh-line expression. The Hugoniot curve is a plot of all the possible values of product specific volumes (1/ρ) and pressures that result from any given values of reactant specific volumes and pressures. The curve represents all the theoretical post combustion states, yet not all of the points on the curve are physically attainable.

To derive the Hugoniot curve, there are four primary equations used to determine the post combustion state thermodynamic properties.

Ideal Gas Law: $$p = \rho RT \quad (1)$$

Conservation of Mass: $$\rho_1 u_1 = \rho_2 u_2 = \dot{m} \quad (2)$$

For a constant area problem, the mass flow rate, $(\dot{m})$ must remain constant.

Conservation of Momentum: $$p_1 + \rho_1 u_1^2 = p_2 + \rho_2 u_2^2 \quad (3)$$

Conservation of Energy: $$C_p T_1 + \frac{1}{2}u_1^2 + q = C_p T_2 + \frac{1}{2}u_2^2 \quad (4)$$

Specific Heat / Gas Constant Relation: $$C_p = \left(\frac{\gamma}{\gamma - 1}\right)R \quad (5)$$

Combining Equation (2) with Equation (3) yields the Raleigh-Line relation, the slope of which is the velocity of the detonation wave.

Rayleigh-Line Relation:
$$\rho_1^2 u_1^2 = \frac{p_2 - p_1}{\frac{1}{\rho_1} - \frac{1}{\rho_2}} = \dot{m}^2 \qquad (6)$$

The Hugoniot Relation can then be obtained by manipulating Equation (4) through the use of Equation (5), and combining the its result with Equations (1) and (2).

Hugoniot Relation:
$$\frac{\gamma}{\gamma - 1}\left(\frac{p_2}{\rho_2} - \frac{p_1}{\rho_1}\right) - \frac{1}{2}(p_2 - p_1)\left(\frac{1}{\rho_1} + \frac{1}{\rho_2}\right) = q \qquad (7)$$

The plot of (p_2) versus $(1/\rho_2)$ for a fixed heat release per unit mass (q), is called the Hugoniot curve and is given in Figure 3.

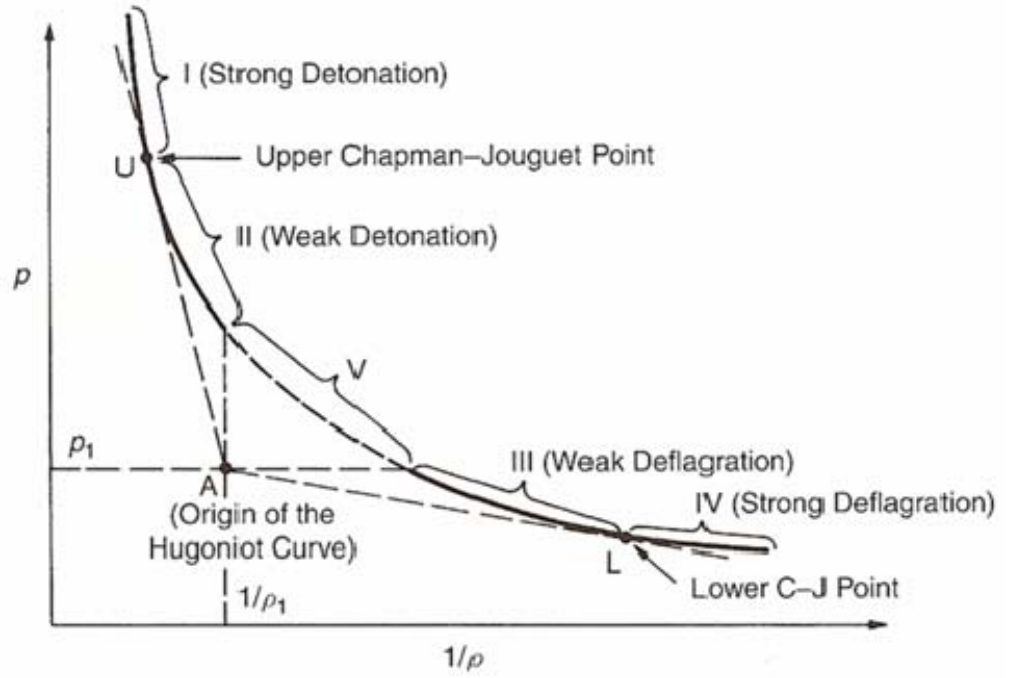

Figure 3. Hugoniot Curve Showing Various Theoretical Combusiton Conditions (From [7])

The intersection of the Rayleigh Lines with the Hugoniot curve divides the curve into regions I through V which indicate the different types of combustion that can theoretically take place. In reality, region V is physically impossible, as it requires

$p_2 > p_1$ and $1/\rho_2 > 1/\rho_1$; conditions that would result in an imaginary velocity (u_1) in the Rayleigh-Line Relation of Equation (6). The Hugoniot curve shows that there are two possible combustion processes; those where the pressure and density decrease (deflagrations) and those where the pressure and density increase (detonations).

The points at which the Hugoniot curve and the Rayleigh lines are tangent are known as the upper (U) and lower (L) Chapman-Jouget (C-J) points. With this understanding, if the Hugoniot Relation of Equation (7) is differentiated with respect to ρ_2 then, Equation (8) is generated.

$$\frac{p_2 - p_1}{\left(\frac{1}{\rho_2} - \frac{1}{\rho_1}\right)} = -\gamma p_2 \rho_2 \tag{8}$$

Then combining Equations (2) and (3) and setting the result equal to Equation (8) yields the relationship;

$$u_2^2 = \frac{\gamma p_2}{\rho_2} = c_2^2 \tag{9}$$

Since $u_2 = c_2$, the upper and lower C-J points represent a condition where the post combustion gas velocity is sonic, even though the detonation wave is moving supersonically into the unburned mixture.

C. THERMODYNAMIC ADVANTAGES OF DETONATIONS

One of the advantageous features of the detonation phenomena is the high thermodynamic efficiency that can be demonstrated. This efficiency can be attributed to two primary factors; the greater cycle efficiency of the Humphrey (PDE) cycle as compared to the more traditional Brayton cycle, and the lower entropy rise relative to deflagration-based processes.

Typical air breathing engines operate by mechanically compressing a fuel-air mixture, combusting (deflagrating) this mixture under near-constant pressure conditions, and then expanding the flow to free-stream static pressure. This cycle is commonly referred to as the Brayton cycle.

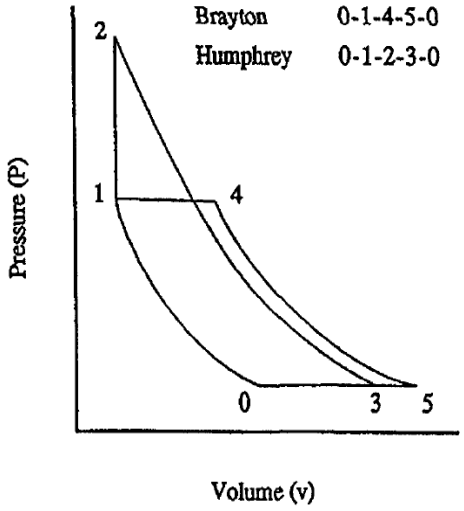

Figure 4. Comparison of Brayton Cycle and a Humphrey Cycle (From [8])

A PDE operates utilizing a Humphrey cycle which is similar to the Brayton cycle (a comparison of these two cycles can be seen in Figure 4), except that the isobaric (1-4) combustion of the Brayton cycle is replaced with a constant volume process (1-2). It should be noted that for a valid comparison, each cycle is assumed to be ideal (optimal isentropic expansion) and that they are both steady state, yet in reality the Humphrey cycle is at best quasi-steady-state. The work performed by each cycle can be determined by integrating the pressure with respect to the volume of their respective curves. A basic inspection of the diagram shows that the Humphrey cycle encloses more area and thus produces more work for a similar heat addition.

Entropy (s) is used as a measure of the useful energy lost in a thermodynamic process. Thus, the lower the rise in entropy due to combustion, the more energy available that can be extracted into useful work and the more thermodynamically efficient the combustion process is. Figure 5 shows the relative values of entropy for the different

regions of the Hugoniot curve. This diagram shows that entropy is at a maximum at the lower C-J point, a deflagration; and that it reaches a minimum at the upper C-J point which represents detonation events. Thus, detonation is inherently more efficient in extracting useful energy from a combustion process [7].

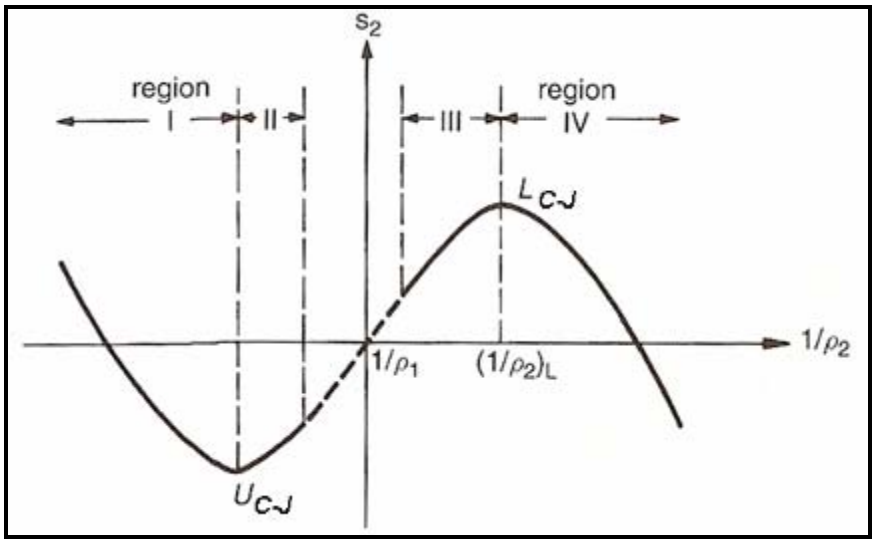

Figure 5. Entropy Distribution on the Hugoniot Curve (From [7])

D. DEFLAGRATION-TO-DETONATION TRANSITION (DDT)

1. Theory

Achieving consistent detonations within the combustor chamber is a mandatory requirement for the successful operation of a PDE. Detonation can be difficult to initiate within fuel and air mixtures in shorter combustor tubes, requiring the application of large amounts of energy. Some of these methods include high-energy ignition, shock focusing, and explosive charges [7].

A more efficient concept is to start a deflagrative combustion and then drive the reaction to a detonation. This process of accelerating the pressure wave into a detonation wave is known as Deflagration-to-Detonation Transition (DDT). DDT begins with a deflagration wave initiated in a reactive mixture by way of a low energy ignition source. The resulting flame front expands as it moves down the combustor, producing pressure

waves ahead of the laminar flame front. Ultimately, the compression waves combine into a single shock front which results in the flame front breaking up due to the turbulence. The turbulent flame has an increased surface area, which in turn increases its reaction and energy release rates. This continues until an "explosion in an explosion" (Figure 6) occurs, creating two shock waves, a superdetonation wave (travelling forward into the unburned gases) and a retonation wave (travelling backward into the combustion products). A spherical shock is also produced, creating lateral shock waves that interact with the superdetonation and retonation waves. After a series of interactions between these multiple shock waves, (Figure 6) a final steady detonation wave is created [7].

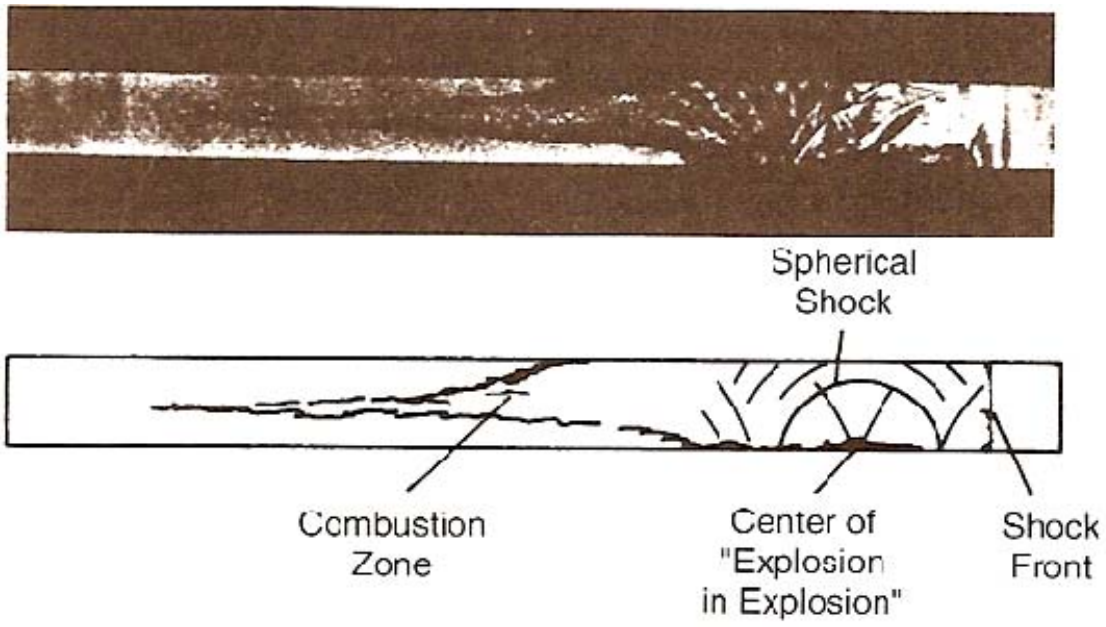

Figure 6. DDT "Explosion within an Explosion" (From [7])

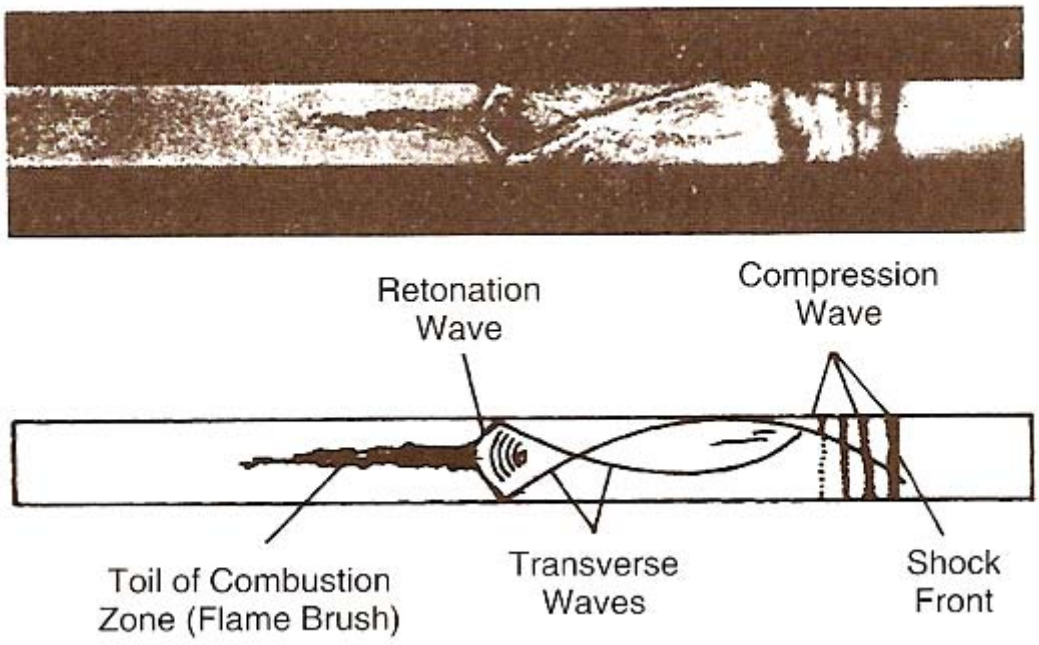

Figure 7. DDT Transverse and Retonation Waves (From [7])

2. DDT Acceleration Using an Obstacle Field

Given a sufficiently long combustor, with a smooth inside surface, DDT can occur due to normal wall roughness and systematic turbulence introduction, leading to high-intensity turbulence in the combustion zone. The use of obstacles in the combustor generates additional turbulence (Figure 8) to the combustion event accelerating the DDT process, and thus allowing it to be completed in a shorter distance than would otherwise be possible without the obstacles. In addition to decreasing the required length of the combustor, obstacle fields increase the repeatability of the DDT process, enhance the shock-generated turbulence, increase the flame surface area, and lead to self-ignition of the fuel ahead of the flame front resulting in an accelerated reaction zone [9].

Most of the historic efforts pertaining to DDT using obstacles have used obstacles with substantial blockage ratios, but recent work at the NPS Rocket Laboratory has shown that modular swept-ramp obstacles, such as those shown in Figure 9, have more favorable performance qualities. They provide effective initiation over short distances

when a fully developed flame condition exists at the entrance to the obstacle field, better thermal management characteristics due to greater contact with the combustor wall (which can be cooled), and a low total pressure loss [6].

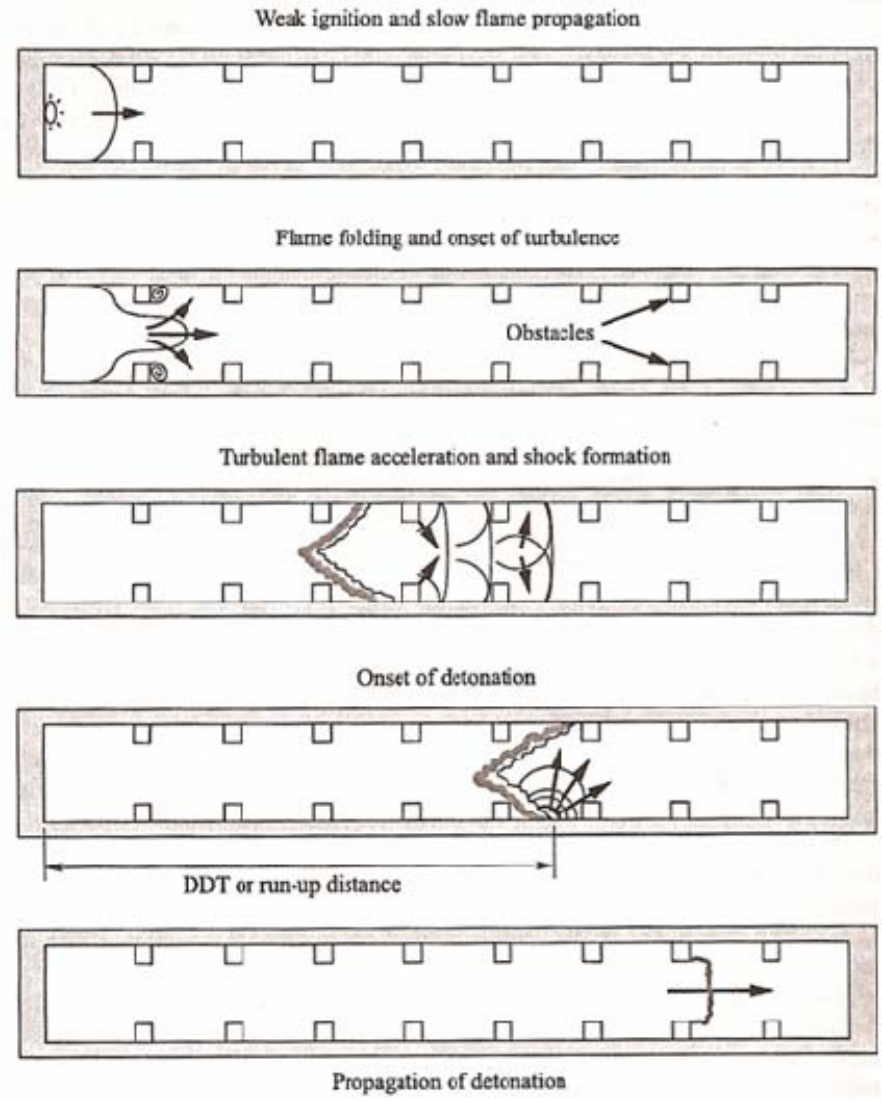

Figure 8. Deflagration-to-Detonation Transition Acceleration in a Tube with Obstacles (From [9])

Figure 9. Ramp Obstacles Tested at NPS Rocket Lab (From [6])

E. PULSE DETONATION ENGINE OPERATION

The combustion cycle of a valve-less pulse detonation engine involves the rapid cyclic loading, detonating, and purging of a combustor. Figure 10 is an illustration of one cycle of a typical detonation process within a closed head-end combustion tube and is described below.

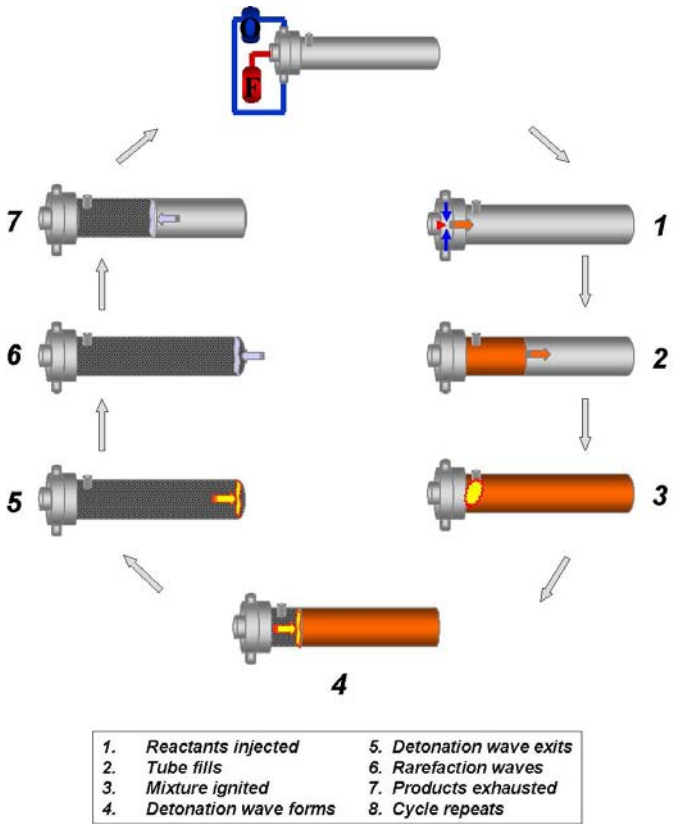

Figure 10. Typical Pulse Detonation Engine Cycle (From [10])

The cycle begins with air entering into the combustor. The fuel and oxidizer are injected and thus mixed into the head end of the combustor (1). The mixture is allowed to fill the combustor (2) and then it is ignited (3), creating a deflagration event in the combustion chamber. The initial deflagration wave propagates down the combustor (4) until a Deflagration-to-Detonation Transition has occurred and a detonation wave is formed. The supersonic detonation wave exits the combustor (5), burning the remaining reactants, and creating a low pressure area inside the initiator and combustor leading to rarefaction waves (6), which rapidly travel back into the PDE venting and exhausting the remaining gases out of the combustor, resulting in thrust (7) and restoring the PDE to the condition in the first frame.

III. DESIGN/EXPERIMENTAL SETUP

Experimental testing was conducted in Test Cell #2 at the Rocket Propulsion Laboratory (RPL), an off-campus testing facility owned and operated by the Naval Postgraduate School (NPS), Monterey, California. A photograph of the test cell is included as Figure 11. A PDC capable of operating using ethylene/air and JP-10/air mixtures was utilized to complete the desired analysis. The PDC geometry was designed and used for previous experimentation; however, in order to evaluate the effects of varying combustor pressure, some modifications, additions, and redesigns were made to the existing system. Modifications were also made to the ethylene and JP-10 fuel delivery systems, a new cooling system was designed and installed, and the combustor section was completely redesigned to withstand the expected pressures and temperatures associated with longer duration operation.

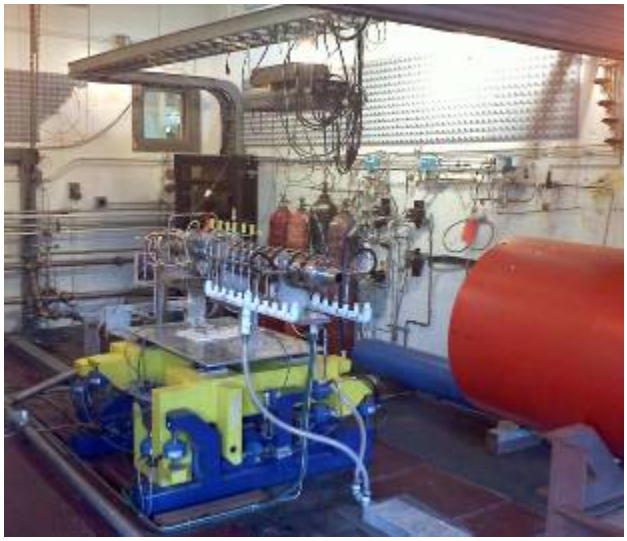

Figure 11. Test Cell #2 at the Naval Postgraduate School Rocket Propulsion Laboratory

A. PULSE DETONATION COMBUSTOR

The NPS PDC is a single tube, “valveless” design that consists of a combustion tube, fuel and air injector systems, an ignition system, and a cooling system. A photograph of the PDC is included as Figure 12.

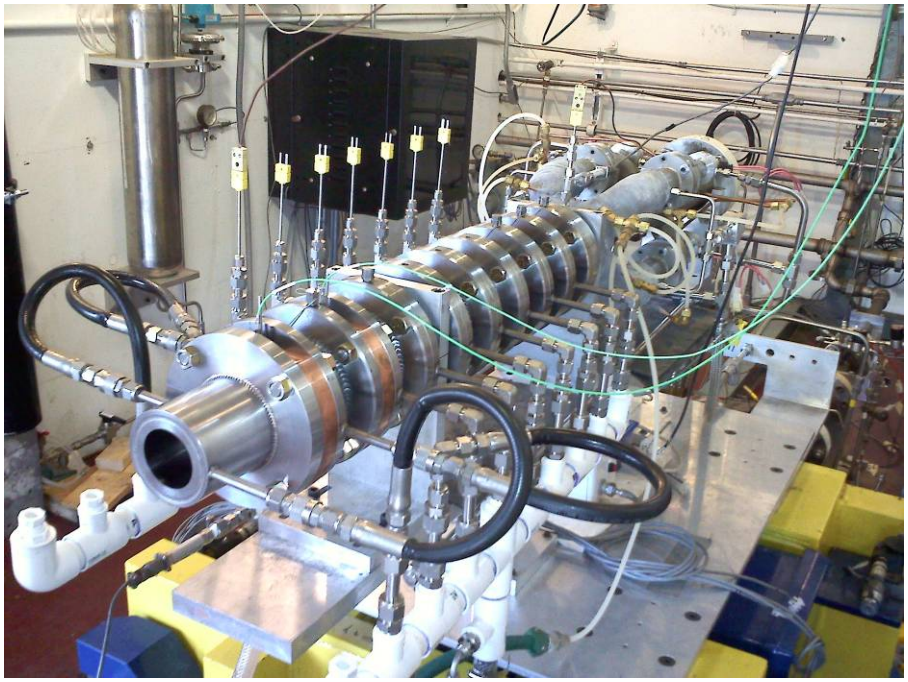

Figure 12. Pulse Detonation Combustor

1. Combustor

The combustor tube was comprised of a number of 3 inch long segments (nominally 9) made from 4340 annealed steel. Each segment consisted of an inner section with channels cut on the backside for cooling water and an outer tube flanged at both ends. An inlet adapter flange was also fabricated to connect a subsequent section and/or the nozzle adapter flange. Figure 13 shows an inner tube from a combustor segment and a complete combustor segment with the inner tube inserted into the outer tube.

Figure 13. Combustor Segment Inner Tube & Complete Combustor Segment

One face of each segment had a 2-243 O-ring groove. Each flange also had holes bored through to the inner tube for the purpose of allowing cooling water to enter and exit the channels of the inner tube and two holes bored through to the inner wall in order to hold obstacles in place with bolts. Detailed schematics of the combustor segments can be found in Appendix B.

The inside diameter of a complete combustor segment and hence the entire combustor section was 3 inches and had attachment points 180 degrees apart for the attachment of obstacles which aided in DDT. A schematic looking up through the combustor toward the inlet is shown in Figure 14; it shows the configuration of the obstacles attached to the inner wall of the combustor. The shape of the obstacle used for all of the testing was the “swept-tall” shape (Figure 15), which was shown to have a good balance between performance and size in previous work at the NPS RPL [6]. The configuration used for all testing was 2R.180.4S and details can be found in Reference [6].

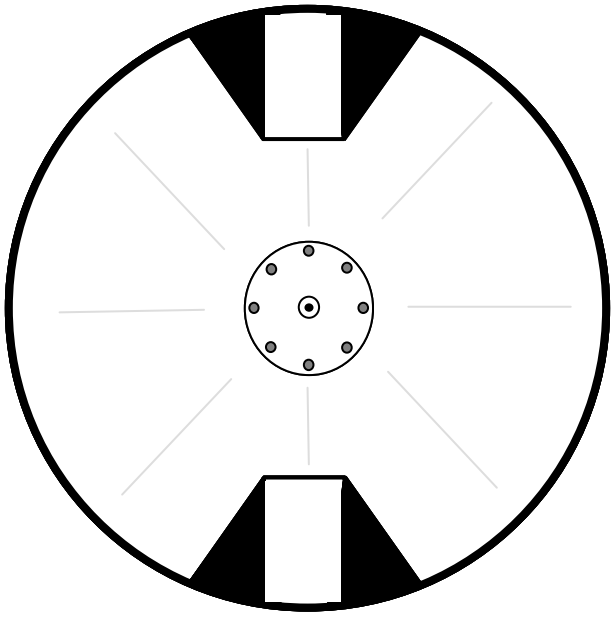

Figure 14. 180 Degree Offset Obstacle Configuration

Figure 15. Swept-Tall Obstacle Shape Used in Testing (From [6])

Adapter flanges were designed that allowed the new combustor segments to connect to the existing inlet and to the existing nozzle. These adapter flanges were made from stainless steel 304 and were ¾ inch thick. The inlet adapter flange also featured a tapered inside diameter which allowed for a smooth transition from the 3.21 inch inner diameter of the existing inlet to the 3.00 inch inner diameter of the new combustor segments. Detailed schematics of the adapter flanges can be seen in Appendix B.

Since the new combustor segments had an increased wall thickness and the addition of water cooling over previous designs, it was necessary to create a new way to measure the change in pressure of the flow and in turn the wave speed. Previous work utilized spark plugs as ion gages while the new design utilized Kistler pressure transducers installed in water-cooled jackets. These will be described further in the "Instrumentation" section. Two spacer rings were designed and installed on either side of the final combustor segment to hold the pressure transducers. The spacers were 7/8 inch thick and made out of Oxygen Free High Conductivity Copper. This material allowed for the maximum conduction of its acquired heat to the surrounding water cooled combustor segments. The spacers utilized the same 2-243 O-ring groove on one side as was used in the combustor segments. The unique design of the spacer, as can be seen in Figure 16, was developed so that the probe could be inserted as close to the inside of the combustor tube as possible while also permitting the spacer to be as thin as possible to minimize the accumulation of heat. A more detailed schematic of the spacers can be seen in Appendix B.

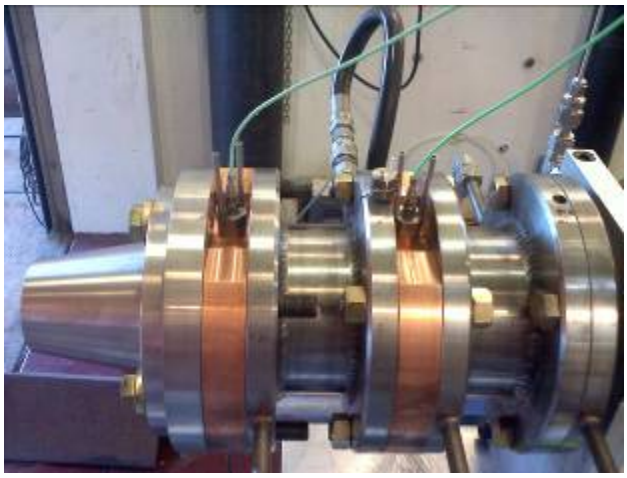

Figure 16. Copper Spacers to hold Pressure Transducers

The entire combustor section of the PDC was made up of a combination of adapter flanges, combustor segments, copper spacers, and a nozzle. Starting at the inlet end, they were arranged in the following order: one adapter flange, three blank (no obstacles installed) combustor segments, five ramp combustor segments, one copper

spacer, one blank combustor segment, one copper spacer, one adapter flange, and one nozzle. The total length of the entire combustor section is thus 30.25 inches, with the nozzle adding an additional 3.625 inches. A schematic of the combustor configuration is shown in Figure 17.

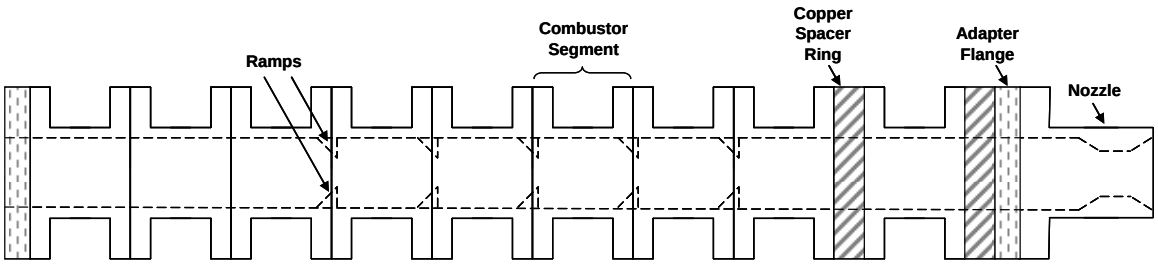

Figure 17. Schematic of Combustor Configuration

2. Fuel Delivery

The fuel delivery system controlled the stoichiometry of the fuel/air mixture that was supplied to the combustor. By varying the pressure of the injected fuel, the mass flow rate ratio of fuel to supply air, known as the equivalency ratio and given by;

$$\varphi = \left[\frac{(F/A)}{(F/A)_{ST}} \right] \tag{10}$$

could be adjusted. In this expression, (F/A) is the mass flow rate ratio of fuel to air for the experimental mixture and $(F/A)_{ST}$ is the mass flow rate ratio of the fuel to air for the stoichiometric mixture. An equivalence ratio near one is indicative of an ideal fuel/air mixture where there is no left over oxidizer or fuel. Specific impulse is the change in momentum per unit of propellant, as given in Equation (11) and (12).

$$I_{SP} = \frac{I_t}{(m_p g_o)} = \frac{F}{(\dot{m} g_o)} \tag{11}$$

$$I_{SP_f} = \frac{F}{\dot{m}_f g_o} \tag{12}$$

An equivalence ratio greater than one indicates more fuel exists than can be combusted with the existing oxidizer. Conversely, insufficient fuel, as would be found when the equivalence ratio is less than one, would result in less than maximum thrust values, but often yields higher fuel-based specific impulses.

The PDE was capable of operating using either an ethylene fuel and its associated injection system or JP-10 and its associated injection system.

a. Ethylene

Ethylene was supplied to the PDE using a newly installed accumulator. The ethylene accumulator (Figure 18) is a cylindrical pressure vessel equipped with a piston. Ethylene was fed into one side from a supply tank and then closed off while nitrogen was fed into the other. The pressure of the nitrogen, and hence the nitrogen side of the accumulator, was controlled with Tescom regulators. By supplying a consistent nitrogen pressure, the piston compressed the ethylene to the desired pressure and forced it into the PDE. This method of using an accumulator allowed for more uniform delivery of the fuel and permitted longer duration operation of the engine.

Figure 18. Ethylene Accumulator

At the PDE, the ethylene was initially supplied into the four fuel arms by a quad injector system. Four electrically-controlled high frequency Valvetech (PN#15060-2) solenoid valve injectors were supplied by a common feed manifold and mounted to the fuel arms downstream of the flow chokes (Figure 19). The gaseous fuel was mixed with the supply air prior to entry into the combustion chamber. As testing progressed to high

chamber pressures, two new fast response Valvetech (PN#12177-2) solenoid valve injectors, which were able to provide about 2.4 times the fuel flow rate of the previous configuration, were installed on the PDE (Figure 20). Each of the two new injectors supplied fuel to two fuel arms, and like the original design, were supplied by a common feed manifold.

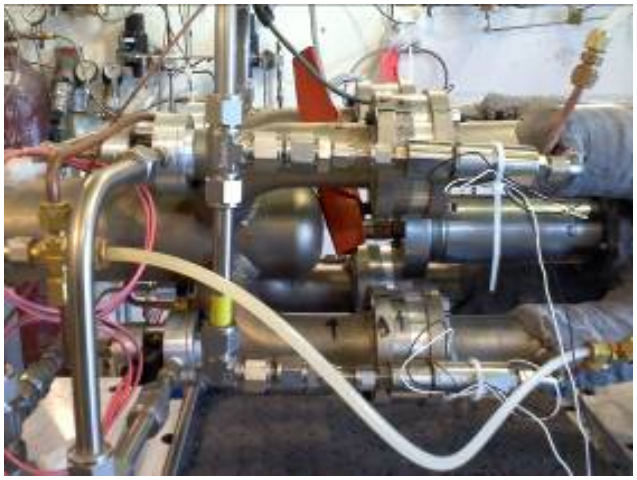

Figure 19. Original Fuel Injectors

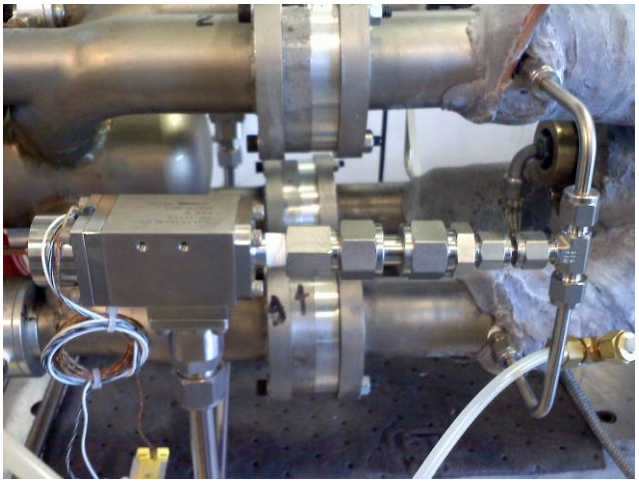

Figure 20. New Fuel Injectors

b. JP-10

In preparation for the operation of the PDE utilizing JP-10, an accumulator, similar in operation to the ethylene accumulator, and with the same fuel delivery benefits, was also installed. The JP-10 accumulator is shown in Figure 21.

Figure 21. JP-10 Accumulator and Pump

Also available for JP-10 delivery was a General Electric 7.5 Hp pump which would independently supply fuel to the PDE. Only one of these systems was used at a time and could be selected via a ball valve. The pump can also be seen in Figure 21.

At the PDC, JP-10 was fed into the four fuel arms with a separate quad injector system. Here, four direct injection-type injectors, fed by a common feed manifold, injected liquid JP-10. Further mixing with the supply air and vaporization occurred as the fuel passed through along the inlet manifold, providing a detonable mixture into the combustor. The injectors can be seen in Figure 22.

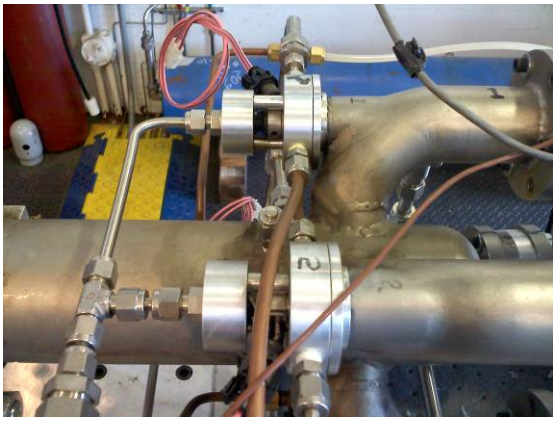

Figure 22. JP-10 Injectors

3. Air Delivery

A constant flow of vitiated air at approximately 380K was delivered from the Hydrogen vitiator (Figure 23) via a 2 inch diameter tube from the supply air subsystem. After entry of the vitiated air into the engine inlet, it was channeled into four 1.5 inch diameter fueling arms (Figure 24), where the fuel was added. This split flow design provided a more uniform fuel/air injection into the combustion chamber. In order to condition the flow prior to entry into the combustion chamber, choked restriction plates were used within each of the fueling arms. These plates also served to isolate the vitiator from downstream pressure oscillations which was necessary to prevent combustor pressure transients from affecting the vitiator flame holding. Later testing removed these plates and relied on one primary air choke that was located just upstream of the vitiator and can be seen in Figure 23.

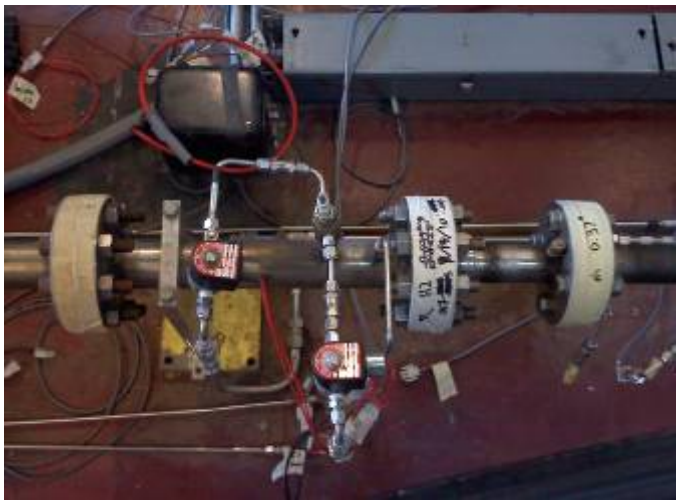

Figure 23. Vitiator Design

Figure 24. PDE Fueling Arms

In order to simulate compressor discharge conditions, such as those found in flight, the air flow into the combustor was heated to approximately 460K using the Hydrogen vitiator. The vitiator was operated for 25–40 seconds prior to the introduction of the fuel which allowed for the heating of the surrounding hardware. This process permitted the incoming air to maintain a nearly constant temperature for a period after the vitiator was shut off. The heating was accomplished by injecting hydrogen into the main air flow and igniting it with a hydrogen/air torch.

4. Ignition System

Ignition was accomplished using a small-scale Transient Plasma Ignition (TPI) system which was previously designed for the NPS PDE. The TPI signal flowchart is illustrated in Figure 23. At the desired operating frequency a BNC 500 Pulse Generator sent a signal to the BNC 575 Pulse/Delay Generator which produced two output waveforms, a trigger and a "rapid charge" input to the High Voltage Pulse Generator. The TPI unit is interfaced with the combustion chamber via an electrode inserted into a machined orifice directly into the combustion chamber. The benefits of this system over other ignition systems had been shown in previous work at the NPS RPL [11].

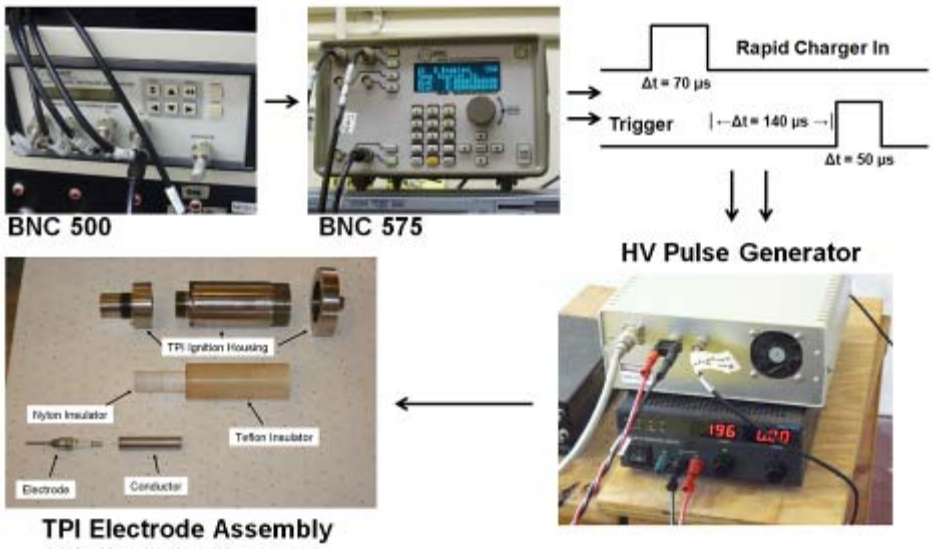

Figure 25. Transient Plasma Ignition (TPI) Equipment and Signal Path (From [6])

The TPI was not designed to operate at higher combustor pressures, and so as testing progressed towards four atmospheres it was necessary to revert to a legacy ignition system. Although this system also used an electrode inserted into the combustor, power was instead supplied from a Unison Vision Variable Ignition System model VIS-2/50 exciter. A Unison Remote Ignition Controller, regulated the application of 1.10 Joules at 20.0 sparks per second to the electrode. The variable ignition system and the controller can be seen in Figure 26.

Figure 26. Remote Ignition Controller & Variable Ignition System

5. Cooling System

Since this work required an increase in the operating pressure of the combustor, it was expected, that the overall heat transfer rates would increase as a result. To prevent damage of the PDE hardware from excessive temperature, a cooling system was employed.

Active cooling of the combustor sections was achieved through the use of a closed-loop water system. Water was supplied from a 115 gallon water storage tank (Figure 27), that was maintained at about 100 gallons. The water was treated with ethylene glycol (automotive antifreeze) in order to reduce the formation of rust on the inside portions of the combustor segments. An MTH brand water pump, Model 284K BF (Figure 28) was used to feed water at about 10 psi, to the combustor segments via a water manifold. The water traveled through the combustor segments and exited on the other side into another central water manifold, and in turn removed heat from the combustor segments. The inlet and outlet water manifolds can be seen in Figure 29. The water was then returned to the water storage tank, to be used again.

Figure 27. Water Storage Tank

Figure 28. Water Pump

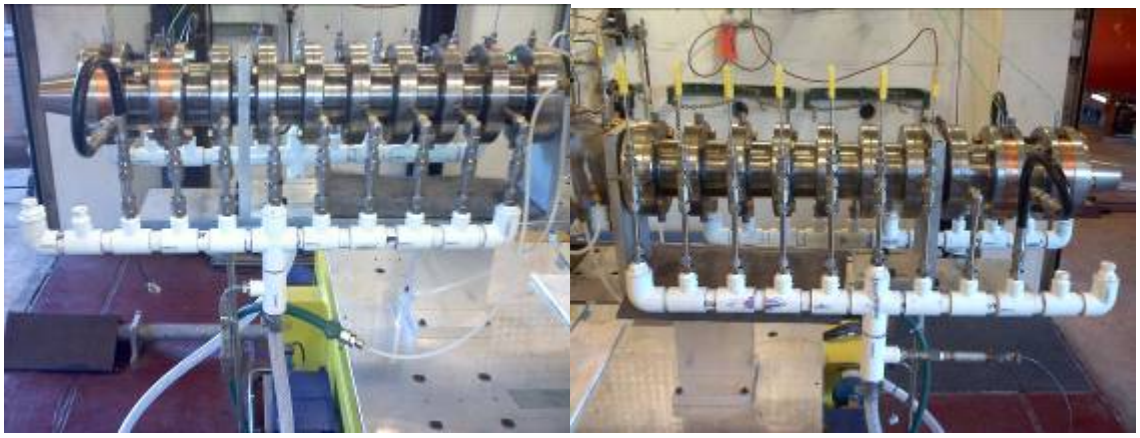

Figure 29. Water Manifolds

Sensors were used on the water manifolds in preparation for further analysis of the temperature differentials across the combustor segments. A temperature and pressure sensor was positioned at the base of the inlet manifold and a temperature sensor was placed prior to the outlet manifold at each combustor segment while the pressure of the outlet flow was measured at the base of the outlet manifold.

Additional cooling was also applied to the fueling arms from a standard shop water line at approximately 30 psig through copper tubing. The tubing was wrapped around the fueling arms and then encased in thermal paste, as can be seen in Figure 24.

B. INSTRUMENTATION

Kistler's Type 603B1 piezoelectric pressure transducers were installed in Kistler's 228P cooling jackets and inserted into the copper spacers. These sensors utilize crystals that, when subjected to mechanical stress, become electrically charged. The charge is exactly proportional to the force acting on the crystal and is measured in picocoulombs (pC). These particular sensors were chosen due their ability to handle transient measurements under extreme high temperatures [12]. A photograph of a pressure sensor next to its cooling jacket is shown in Figure 30.

Figure 30. Kistler Pressure Sensor and Kistler Cooling Jacket

The pressure sensors output a 0–10 signal when a pressure wave passes by the measurement locations. The distance between the sensors is known to be 3.875 inches. By measuring the elapsed time between the pressure spikes the wave speed can then be

calculated to ensure detonation was achieved. Wave speeds found in excess of 1500 m/s were considered to be indications of detonation.

The charge signals of the sensors were sent from the pressure transducers to Kistler's Type 5010 multi-range charge amplifiers, which converted and amplified the signals to a proportional voltage. The sensitivity of the amplifiers was set to 0.380 pc/MU and the scale was set to 100 MU/volt. A photograph of the amplifiers used for testing is given in Figure 31.

Figure 31. Kistler Amplifiers

After the signal was amplified it was sent to National Instrument's BNC-2090 rack-mounted analog breakout accessory, shown in Figure 32. This accessory simplifies the connection of analog signals and digital signals to the data acquisition system.

Figure 32. National Instruments BNC-2090

C. DATA ACQUISITION

Data acquisition was controlled by the LabView Graphical User Interface as shown in Figure 33. This software program was operated from a computer in the control

room. The "Start Data Recording" button was selected at the same time as the ignition system was initiated and in turn recorded three seconds of pressure data from the pressure transducers. Precursory analysis of the data was possible directly in the Labview program, but the data was also deposited into a file folder for further post-test analysis using Matlab.

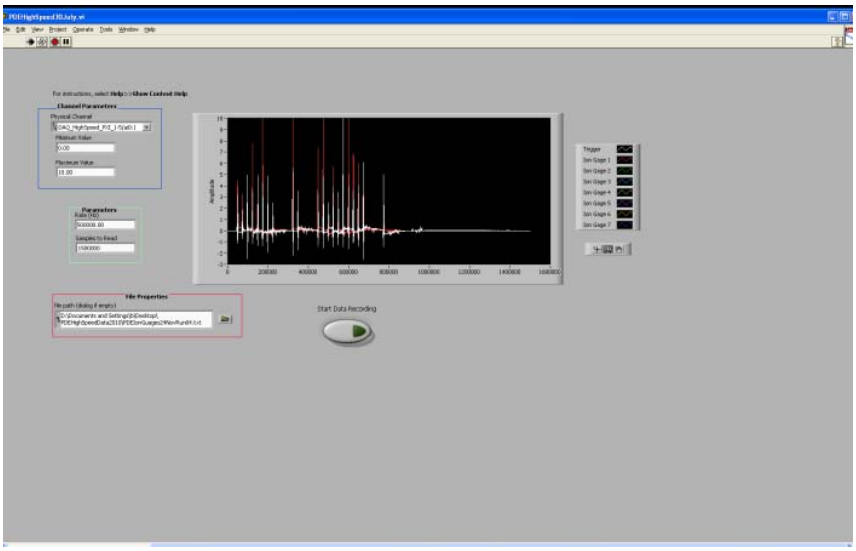

Figure 33. LabView Data Acquisition Controller

D. PDE CONTROLLER SOFTWARE AND PROCEDURE

The PDE was controlled by National Instruments (NI) Labview programs installed on two computers in the control room of the RPL. One computer was linked to a NI PXIe-1062Q controller and the other was linked to a NI PXI-1000B controller. Together these programs controlled the operation of the engine by cycling gas supply valves located in the test cell and controlled the event sequencing. For safety purposes, emergency shutoff buttons were linked to each system and available within the control room. These buttons were capable of closing all supply gas valves and interrupting fuel injection and ignition trigger signals, and thus disabling the test cell. The Labview Graphical User Interfaces used to control the PDE are shown in Figures 34 and 35.

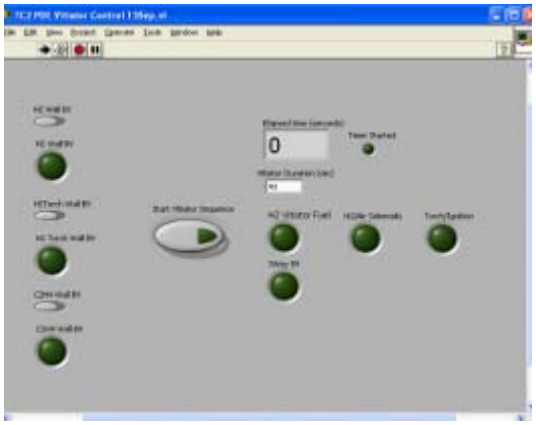

Figure 34. Labview Interface Controller 1

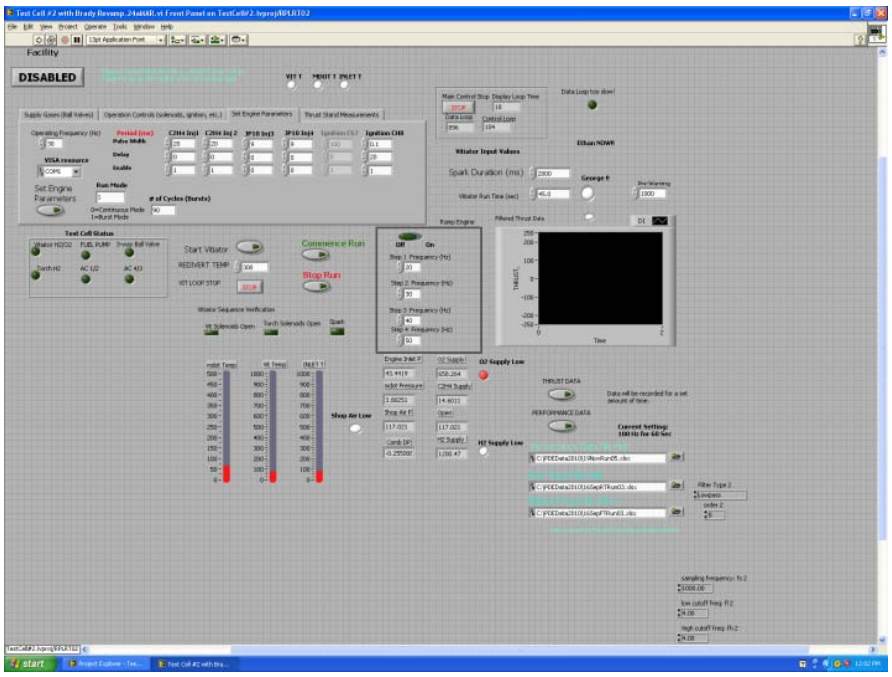

Figure 35. Labview Interface Controller 2

The PDE was prepared prior to operation and operated using a systematic procedure in order to ensure safety and minimize the number of faulty runs. These Standard Operating Procedures are provided in Appendix A.

IV. EXPERIMENTAL RESULTS

Testing was conducted utilizing the new combustor at combustor pressures between two and five atmospheres and with initial temperatures between 390–450°F. The combustor was operated at 20 Hz and for 30 cycles or 1.5 seconds in duration. A schematic of the typical scheduling for one cycle at 20 Hz is given in Figure 36. At each pressure, detonability was evaluated across an equivalency ratio range of about 0.9–1.1. Also, as the pressure was increased, ramp "stations" used for DDT were removed to determine the minimum number of ramps that would still allow for DDT at each pressure. It was expected that as the pressure increased, DDT would occur with fewer ramps. It should be noted that when the reduction from five ramps to four took place, the combustor segment that they were attached to was also removed, in turn reducing the length of the combustor by three inches.

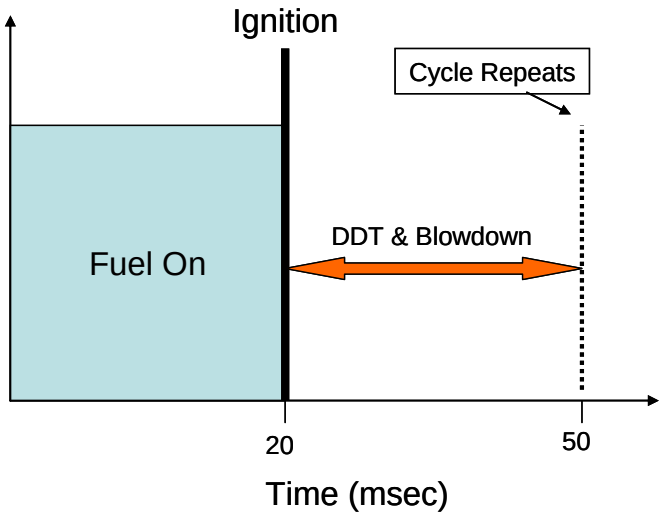

Figure 36. Typical Scheduling for 1 Cycle at 20 Hz

In general, the 107 "runs" completed for this research were conducted by setting the fuel and air pressures for the desired equivalency ratio and then operating the PDC. The precursory analysis of the Kistler probe data in the Labview program allowed for the almost immediate determination if detonation (a wave speed greater than 1,500 m/s) had

occurred or not. After looking at the test data, a degradation of one of the Kistler probe signal lines prevented the confirmation of some detonation events when in fact it was believed they had occurred. Therefore, for the purpose of this research, if more than 50% of the valid pulses were a detonation, then the run, and in turn the applied equivalency ratio, was taken to be a successful detonation condition.

In an effort to evaluate only the effect that an increased pressure would have on the PDC, many parameters were held constant throughout all pressure regimes and are given in Table 2. Parameters that varied across the different pressures and configurations are given in their associated section.

Frequency	Duration	Fuel Timing
20 Hz	1.5 sec	20 msec

Table 2. Common PDC Parameters Across All Pressures

A. RUNS AT 2.5 ATMOSPHERES

Preliminary testing up to two atmospheres had been conducted on the previously designed PDC at the RPL with satisfactory results. The current effort initially began with the new combustor operating at 2.5 atmospheres of combustor pressure. The parameters that were used are given in Table 3.

Main Air Choke	Mass Flow Rate of Air	Combustor Refresh Conditions	
		P_{INIT}	T_{INIT}
0.370 in	1.763 lb_m/s	2.5atm	450°F

Table 3. Run Conditions 2.5 Atmospheres

1. First Sequence (5 Ramp Sets)

In the first sequence, the combustor was configured with five sets of ramps and eight runs were completed. Detonation for this sequence occurred using fuel pressures from 575–650 psi or an equivalency ratio of 0.85–0.96. An example of a successful

detonation run at an equivalency ratio of 0.92 is given in Figure 37 and an enlarged view of one of the detonation pulses showing the shock wave registering at each pressure transducer is given in Figure 38.

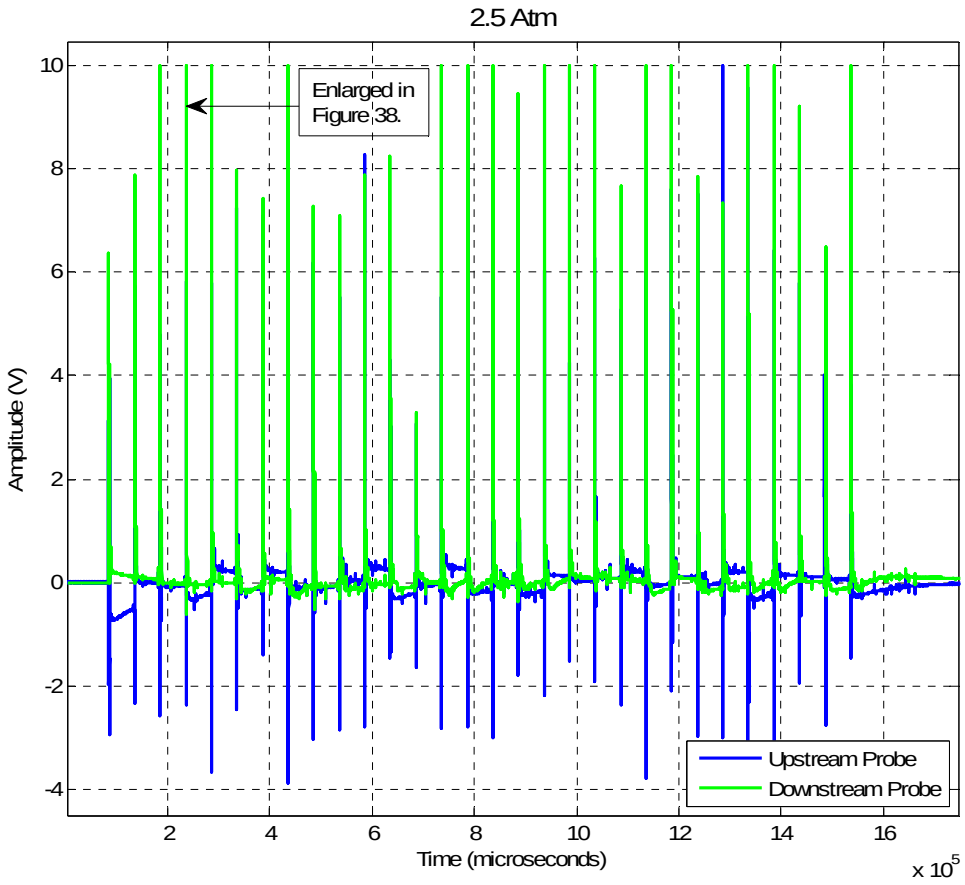

Figure 37. Pressure Transducer Data - 2.5 Atmospheres; 0.92 Equivalency Ratio; 5 Ramp Sets; Detonation Achieved

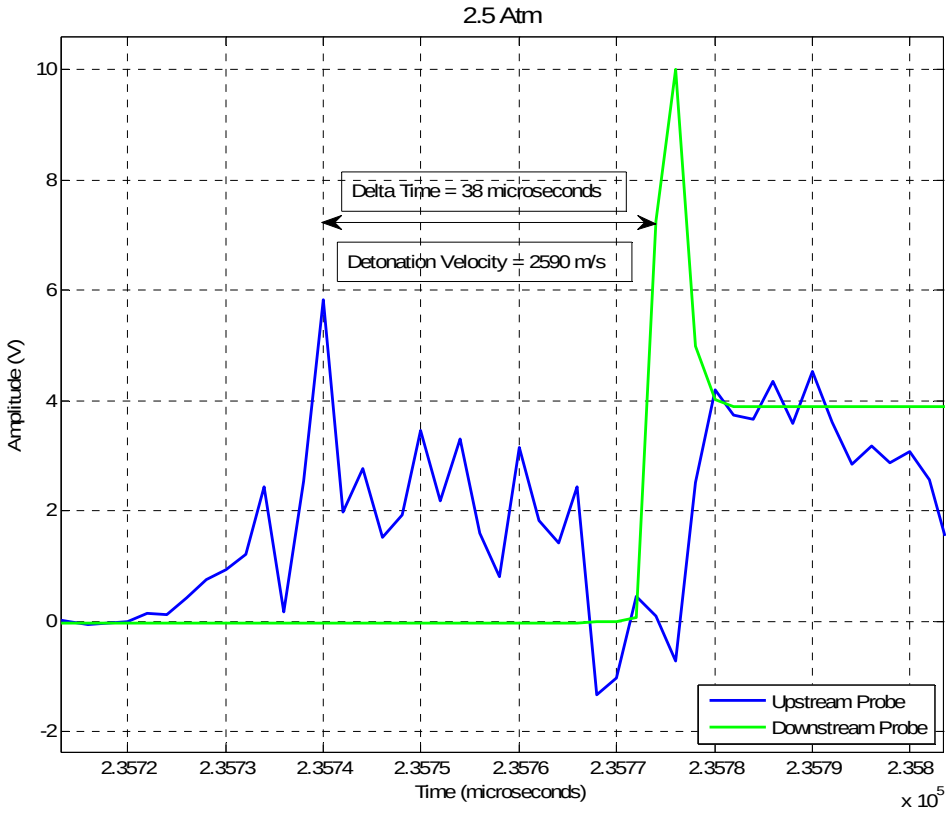

Figure 38. Enlarged View of a Detonation Peak from Figure 37

2. Second Sequence (4 Ramp Sets)

The second sequence at 2.5 atmospheres included twelve runs and utilized four ramp sets. The same parameters from the first sequence were still used as given in Table 3.

Detonation for this sequence occurred using fuel pressures from 620–665 psi or an equivalency ratio of 0.91–0.98.

B. RUNS AT 3.3 ATMOSPHERES

At this point the new ethylene Valvetech injectors were installed to allow for greater fuel flow rates which were necessary for operation at higher pressures. A series

of runs were conducted in order to calibrate them properly and determine if the calculated increase in fuel flow rate of 2.4 times was a realistic value.

1. First Sequence (4 Ramp Sets)

After 34 runs, all still utilizing 4 sets of ramps, testing revealed experimentally that in fact the new injectors were supplying about 1.57 times the fuel flow as the old injectors. The parameters used for the 3.3 atmosphere case are given in Table 4.

Main Air Choke	Mass Flow Rate of Air	Combustor Refresh Conditions	
		P_{INIT}	T_{INIT}
0.370 in	1.056 lb_m/s	3.3 atm	450°F

Table 4. Run Conditions 3.3 Atmospheres

Similar to the 2.5 atmosphere case, detonations for this pressure setting occurred when the equivalency ratio was between 0.91 and 0.98. An example of a successful detonation run at an equivalency ratio of 0.96 is given in Figure 39 and an enlarged view of one of the detonation pulses showing the shock wave registering at each pressure transducer is given in Figure 40.

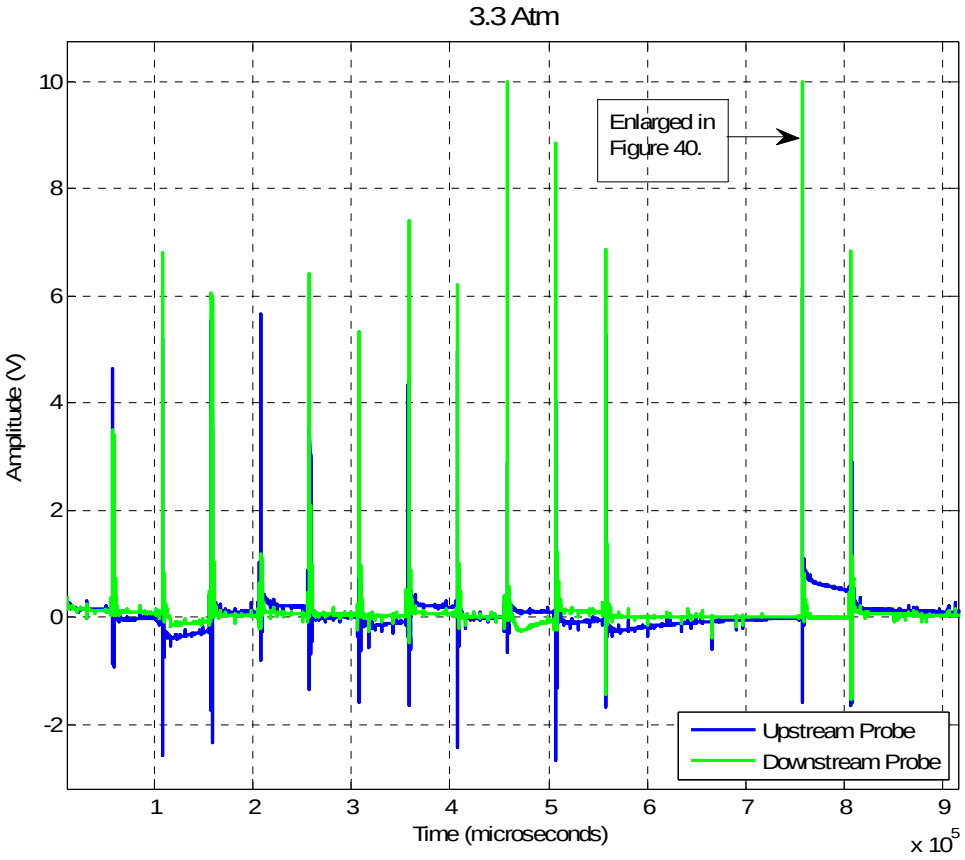

Figure 39. Pressure Transducer Data - Enlarged View; 3.3 Atmospheres; 0.96 Equivalency Ratio; 4 Ramp Sets; Detonation Achieved

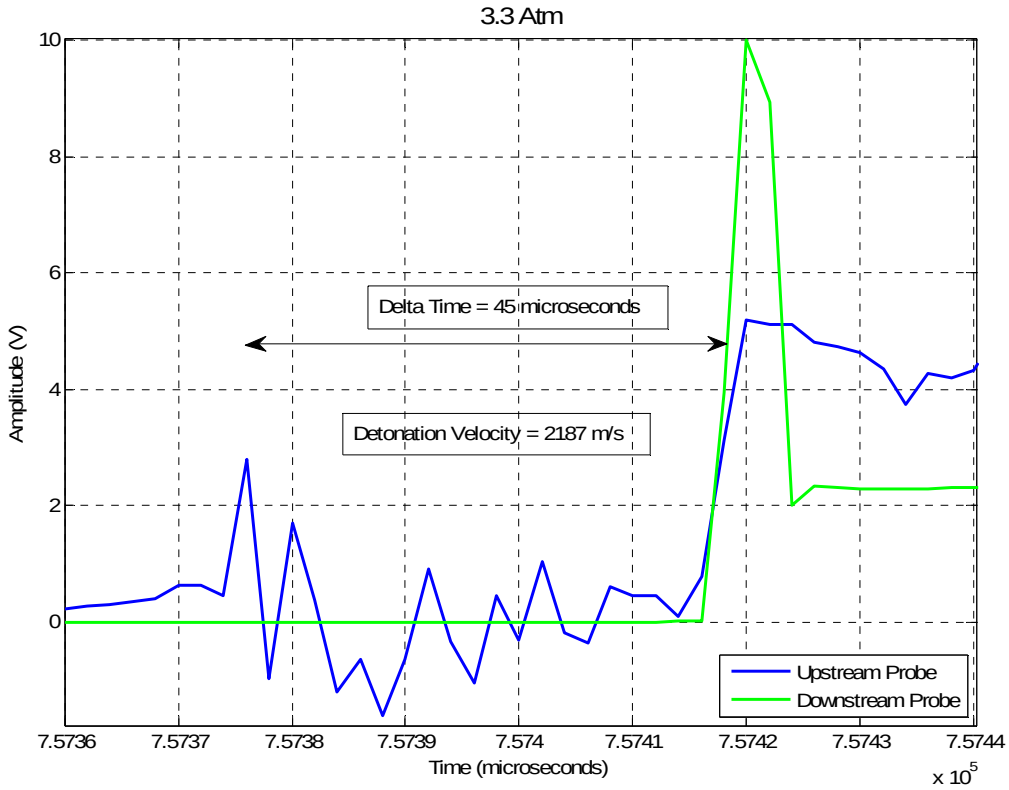

Figure 40. Enlarged View of a Detonation Peak from Figure 39

2. Second Sequence (3 Ramp Sets)

The second sequence in the 3.3 atmosphere regime saw the removal of another set of ramps, leaving the combustor with three sets of ramps. Following the nomenclature of Reference 6, this configuration is considered as 2R.180.3S. Even though the range of fuel pressures that had produced the strongest detonations in the first sequence, were used, only partial detonations (up to 40%) were observed in this configuration. This data indicates that at least four sets of ramps are necessary for detonation at this pressure and temperature. Figures are omitted as they were not considered successful detonations.

C. RUNS AT 4.0 ATMOSPHERES

Four atmospheres in the combustor was achieved by using the parameters given in Table 5 and a fuel pressure range of 475–525 psi. Unfortunately ignition was not even taking place, let alone detonation. It was determined that the TPI system, which was not

specifically designed for operation at higher pressures, may be the reason for the lack of ignition.

Main Air Choke	Mass Flow Rate of Air	Combustor Refresh Conditions	
		P_{INIT}	T_{INIT}
0.370 in	1.28 lb_m/s	4.0 atm	450°F

Table 5. Run Conditions 4.0 Atmospheres

The Unison Variable Ignition System was installed and ignition adjusted for the new ignition system. No detonations were observed over the equivalence ratios investigated.

D. RUNS AT 5.0 ATMOSPHERES

Five atmospheres were achieved by increasing the main air choke and appropriately scaling the parameters as given in Table 6. Time constraints permitted only three runs and although no detonations were achieved, one of the runs at a 1.17 equivalency ratio contained a partial detonation.

Main Air Choke	Mass Flow Rate of Air	Combustor Refresh Conditions	
		P_{INIT}	T_{INIT}
0.435 in	1.60 lb_m/s	5.0 atm	450°F

Table 6. Run Conditions 5.0 Atmospheres

E. SUMMARY

A summary of the results from all the different configurations is given as Table 7. In the table, the green shading indicates a configuration that had 50% or greater detonations per valid pulse, while the yellow indicates a configuration where detonations made up 20% to 50% of the valid pulses. Finally, red shading indicates that detonation did not occur for a given configuration. This table is not an indication of the number of

runs completed for any given configuration, but is rather an effort to supply some brevity to a comprehensive data file by "averaging" any duplicated configurations across the runs.

Combustor Refresh Pressure	Injectors	Ignition System	Ramps	Equivalence Ratio
2.5 Atm	Valvetech 15060-2 (x4)	TPI	5	0.81
				0.85
				0.92
				0.96
				0.99
				1.03
			4	0.89
				0.90
				0.91
				0.93
				0.96
3.3 Atm	Valvetech 12177-2 (x2)			0.81
				0.87
				0.88
				0.90
				0.92
				0.98
				0.99
				1.02
			3	0.90
				0.92
				0.95
				0.97
				0.99
				1.02
				1.04
4.0 Atm				1.00
				1.02
				1.04
		Unison CD		0.94
				0.96
				0.98
				1.00
				1.02
				1.04
5.0 Atm				1.17
				1.21

Key	
	>50% Detonations
	20 - 50% Detonations
	No Detonations

Table 7. Summary of Experimental Results

THIS PAGE INTENTIONALLY LEFT BLANK

V. CONCLUSIONS

In order to realize the thrust and power generation applications of PDCs, it will be necessary to operate them at higher combustor pressures. As the pressure increases, the detonation cell size of the fuel/air mixture decreases, and in turn enhances the susceptibility of the mixture to undergo detonations. This effort investigated the detonation initiation requirements associated with the operation of a PDC at higher pressures. The design of the cooling combustor, the cooling nozzle, and their associated water cooling system allowed the PDC to successfully operate over long run durations. Improved Valvetech injectors for the ethylene were installed and a new ethylene accumulator was shown to adequately supply the necessary fuel flow rates. Pressure transducers used to determine detonation wave speed were also designed with the option of active cooling for heat dissipation.

The operation of the PDC for this thesis work revealed that for near-stoichiometric ethylene/air mixtures, detonations can be achieved when using four sets of the tall-swept ramp geometry (2R.180.4S) at 3.3 atmospheres and below. The reduction of the ramp sets down to three did not produce any detonations and will likely require combustor pressures higher than 5 atmospheres.

THIS PAGE INTENTIONALLY LEFT BLANK

APPENDIX A: PULSE DETONATION ENGINE STANDARD OPERATING PROCEDURES

Standard Operating Procedures

Test Cell #2

Modification Date (29 October 2010)

RUN Setup Procedures

1. Lab Personnel – NOTIFY OF IMPENDING TEST
2. Gate – LOCK
3. Warning Lights – ON
4. Air Bank Pressure – CHECK >1500 psi
5. Run Sheet – COMPLETE
    a. Required pressures – NOTE
6. On TC#3 Computer (32-bit)
    a. "TC2 PDE Vitiator Control 15 Sep" – OPEN & RUN
    b. "PDE High Speed 27 July" (in PDE High Speed Folder) – OPEN & RUN
    c. Data File – CHANGE NAME
        i. Right click data file, select "Data Operations," select "Make Current File Default," File – SAVE
7. On TC#2 Computer (32-bit)
    a. "National Instruments Lab View" – OPEN
    b. "Test Cell #2.lvproject" – OPEN
    c. Maximize tree by clicking + symbol
    d. "Test Cell #2 with Brady Revamp.24aMAR.vi" – OPEN & RUN
    e. Run Sheet Values – ENTER
    f. "Set Engine Parameters" – SELECT
    g. Data File – CHANGE NAME
        i. Right click data file, select "Data Operations," select "Make Current File Default," File – SAVE
8. Emergency Stop Buttons (x2) – IN
9. 5V Power Supply – OFF
10. BNC Cabinet Power Strip – ON
11. BNC Box (on top of cabinet) – ON
    a. CH. A (0.00007 / 0.0) – VERIFY (set with TC#2 computer)
    b. CH. B (0.00005 / 0.00021) – VERIFY (set with TC#2 computer)
12. Gas pressure on Node 22 (N_2) to ~300psi to prevent excessive venting – SET

Outside

13. Jamesbury Valve – OPEN
14. Node 4 Ball Valve (in TC#1) – OPEN
15. H2 Six Pack – CHECK PRESSURE & OPEN

16. DAQ Power (in TC#3) – ON
17. At Overhead Boxes (in TC#2)
    a. Power Supply – ON (170 volts)
    b. TPI – ON
18. Vitiator Spark Plug – DISCONNECT
19. Main Air (yellow handle) – CLOSE
20. Water Valve – OPEN
21. Shop Air (red handle) – OPEN (can verify with blue handle)
22. Node 4 Isolation Valve – OPEN
23. Transducer TESCOM Power – ON
24. Kistler Amplifiers – ON and OPERATE
25. Tank Opening (when using blue accumulator)
    a. Ethylene Ball Valve – OPEN
        i. Check C_2H_4 pressure in accumulator and note if sufficient. If NOT sufficient perform accumulator fill procedures
    b. N_2 Ball Valve – OPEN
    c. H_2 – OPEN
    d. H_2 Torch – OPEN
    e. N_2 Tank – OPEN
26. Cooling Water Pump
    a. Test Cell #3 Knife Switch – ON
    b. Knife Switch Breaker Handle – ON
    c. Water Tank – CHECK (full and clean)
    d. Water Tank Isolation Valve – OPEN
    e. Test Cell #2 Ball Valve – OPEN (ensure TC#3 valve closed)
27. Shop Air Tank (closet) – CHECK (95-120 psi)

Inside

28. Set Gas Pressures (in control room)
    a. Node 1; Main Air
    b. Node 4; High Pressure Air
    c. Node 20; Vitiator H_2
    d. Node 22; C_2H_4 controlled with N_2
29. 24 volt DC – ON (check with other test cells prior)
30. BNC Box – RUN
31. Main Air (yellow handle) – OPEN
32. Vitiator Spark Plug – CONNECT

**********TEST CELL DANGER CONDITON**********

Run Profile

1. Personnel – HEAD COUNT
2. Labview Programs – MODIFY FILE NAME AS NECESSARY & RUN
3. Golf Course – CLEAR

4. Siren – ON
5. Emergency Stop Buttons (x2) – OUT
6. 5V Power Supply – ON
7. Valves
    a. H_2 Wall – OPEN
    b. H_2 Torch – OPEN
    c. C_2H_4 Wall – OPEN
8. Main Air – ON
9. Cooling Water – ON
10. Vitiator – START
11. Countdown
12. Bottom BNC Controller – START (When Inlet Temperature (390-400); H_2 Vitiator Fuel Light is On)
13. Data Recording – START

<u>After Run</u>

1. 3-Way Ball Valve Light – OFF (Wait for main air to divert)
2. Cooling Water – OFF
3. Main Air – OFF
4. Siren – OFF
5. Valves
    a. H_2 Wall – CLOSE
    b. H_2 Torch – CLOSE
    c. C_2H_4 Wall – CLOSE
6. Emergency Stop Buttons (x2) – IN
7. 5V Power Supply – OFF

<u>Run Shutdown Procedure</u>

1. Valves
    a. H_2 Wall – CLOSE
    b. H_2 Torch – CLOSE
    c. C_2H_4 Wall – CLOSE
2. Emergency Stop Buttons (x2) – VERIFY IN
3. 5V Power Supply – VERIFY OFF
4. Set Gas Pressures
    a. Node 1 – ZERO
    b. Node 4 – ZERO
    c. Node 20 – ZERO
    d. Node 22 – MAINTAIN CURRENT VALUE (consider minor reduction)
5. BNC Cabinet Power Strip – OFF
6. BNC Box – OFF
7. 24 volt DC – OFF (check with other test cells prior)
8. Jamesbury Valve – CLOSE

9. Node 4 Ball Valve (in TC#1) – CLOSE
10. At Overhead Boxes (in TC#2)
    a. TPI – OFF
    b. Power Supply – OFF
11. Vitiator Spark Plug – DISCONNECT
12. Main Air (yellow handle) – CLOSE
13. Water Valve – CLOSE
14. Shop Air (red handle) – CLOSE
15. Bleed Shop Air (blue handle) – OPEN then CLOSE
16. Node 4 Isolation Valve – CLOSE
17. Kistler Amplifiers – OFF
18. Transducer TESCOM Power – OFF
19. Tanks (with accumulator)
    a. H_2 – CLOSE
    b. H_2 Torch – CLOSE
    c. N_2 – CLOSE
20. Cooling Water Pump
    a. Test Cell #2 Ball Valve – CLOSED
    b. Water Tank Isolation Valve – CLOSED
    c. Knife Switch Breaker Handle – OFF
    d. Test Cell #3 Knife Switch – OFF
21. DAQ Power (in TC#3) – OFF
22. H2 Six Pack – CLOSE & RECORD PRESSURES
23. Warning Lights – OFF

APPENDIX B: COMPONENT DRAWINGS

A. COMBUSTOR SECTIONS

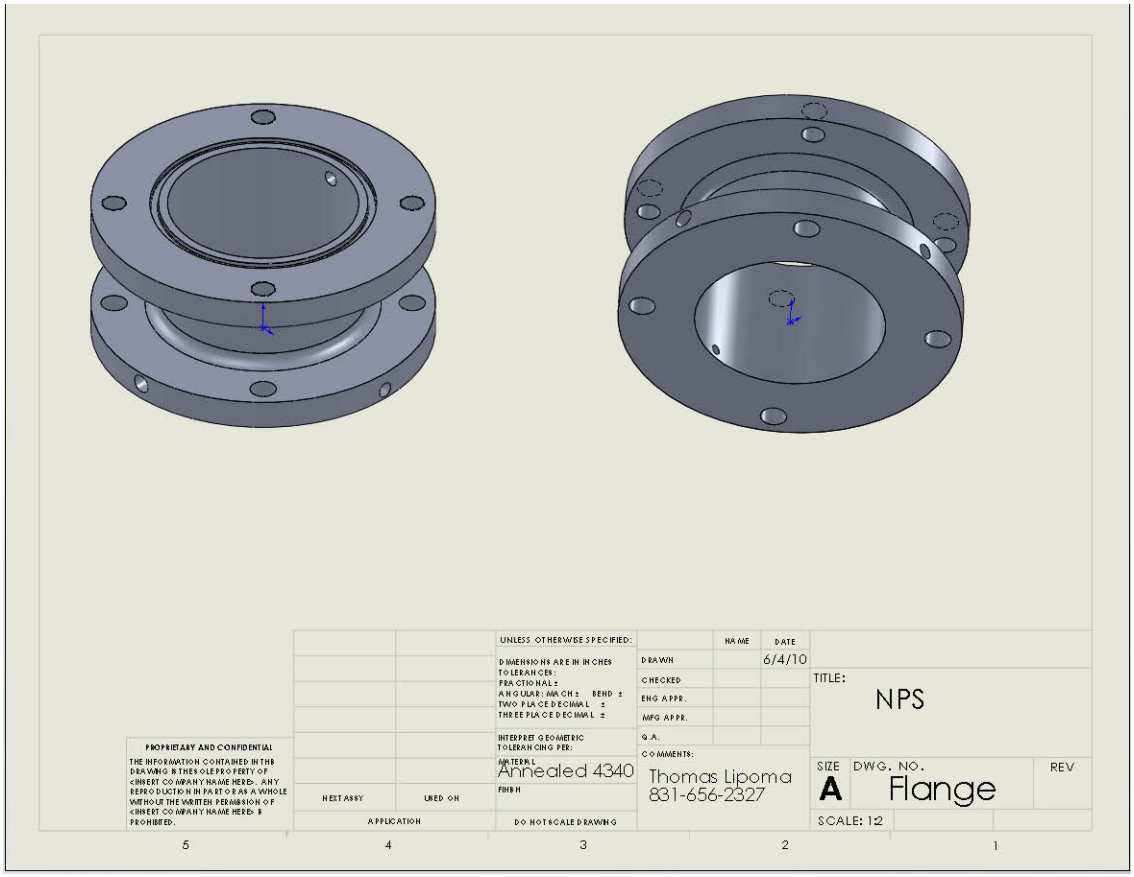

Figure 41. Combustor Sections – Isometric View

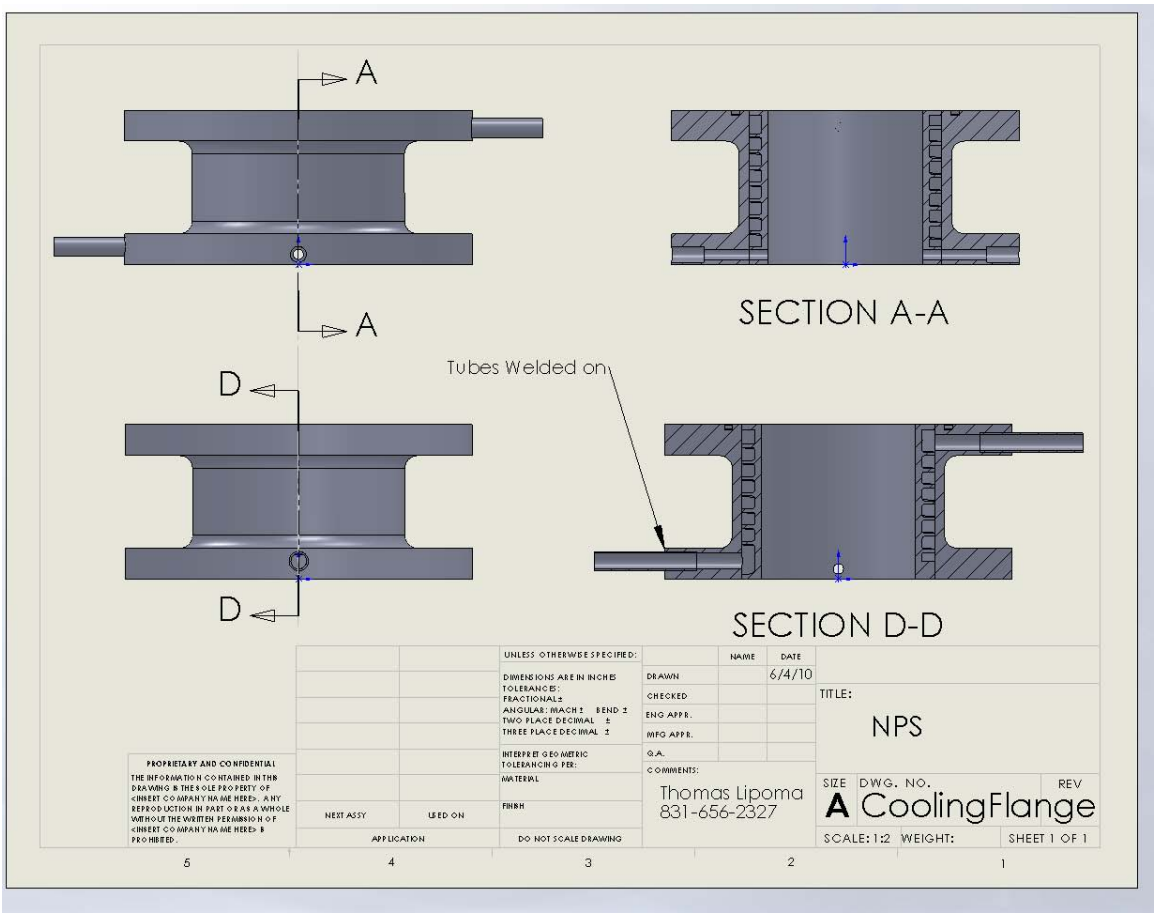

Figure 42. Combustor Sections – Plan View

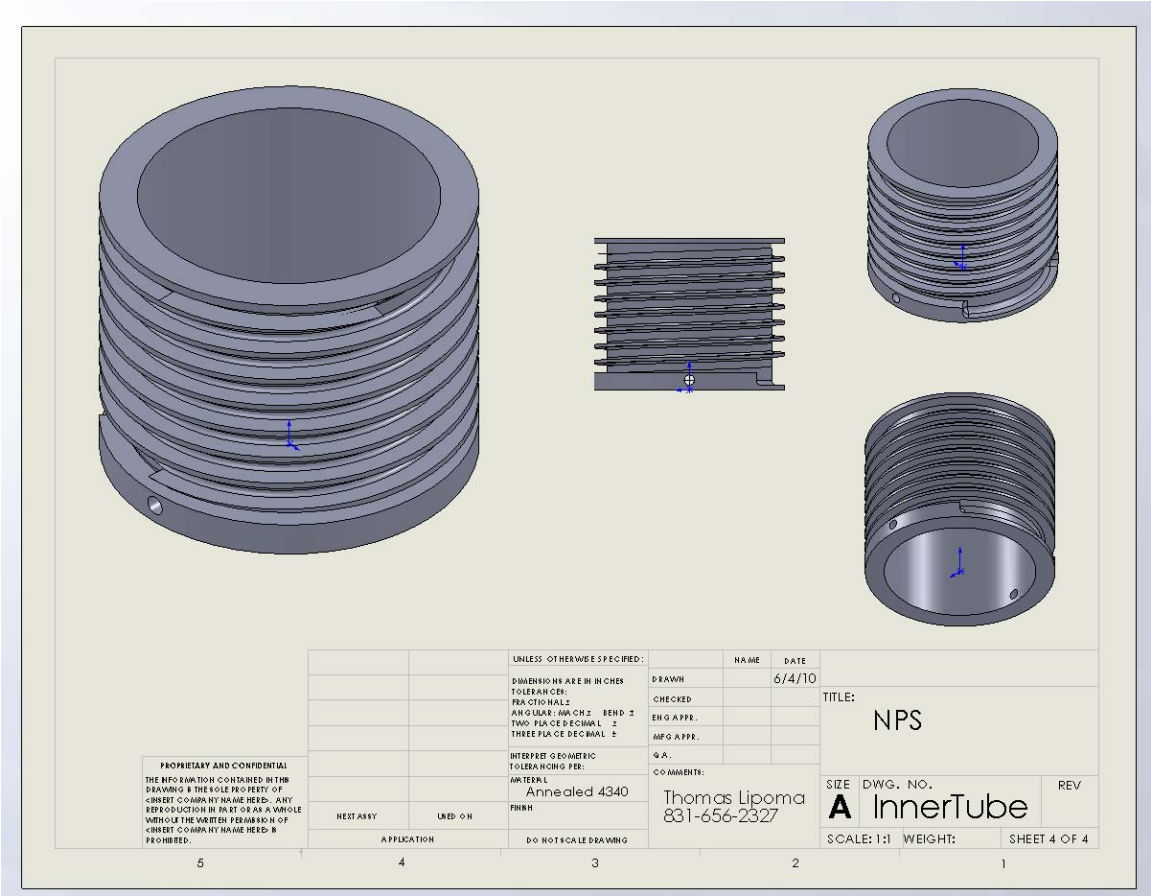

Figure 43. Combustor Sections – Inner Tube

B. COOLING NOZZLE

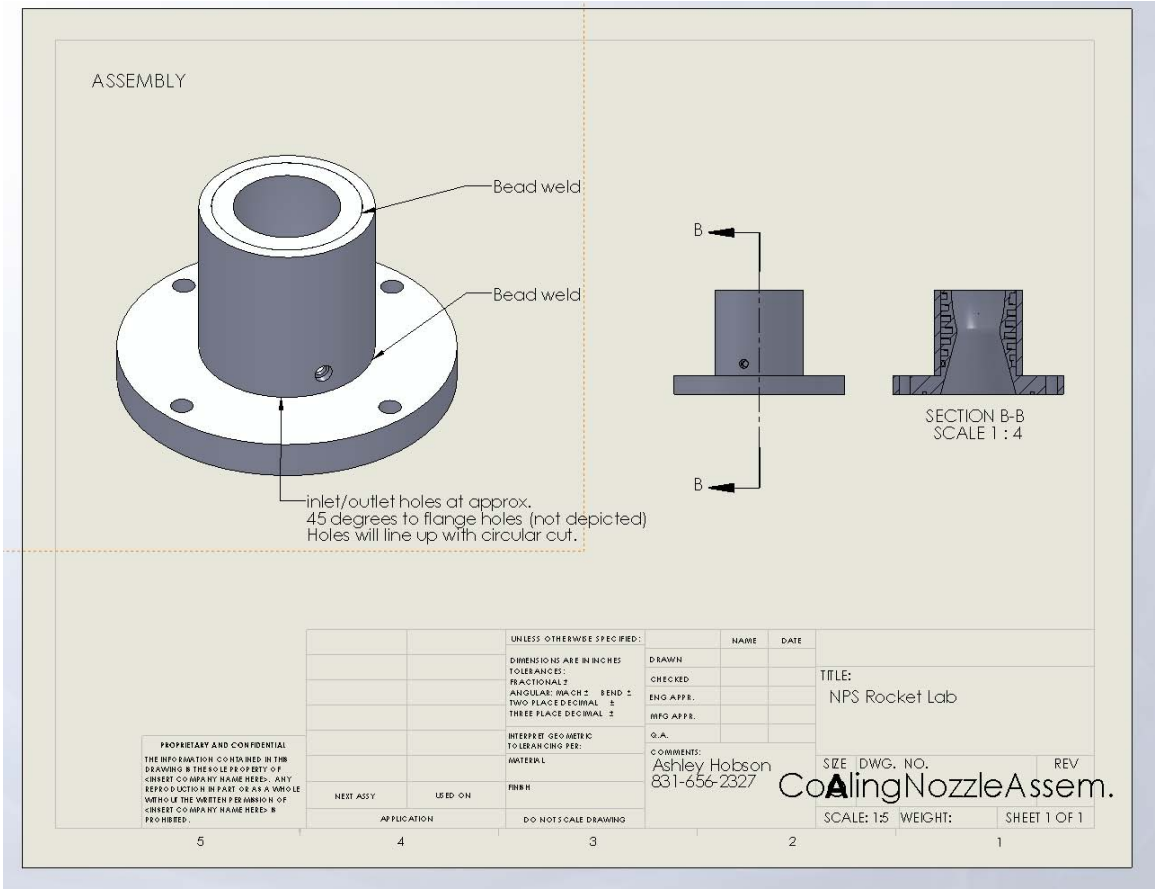

Figure 44. Cooling Nozzle – Assembly

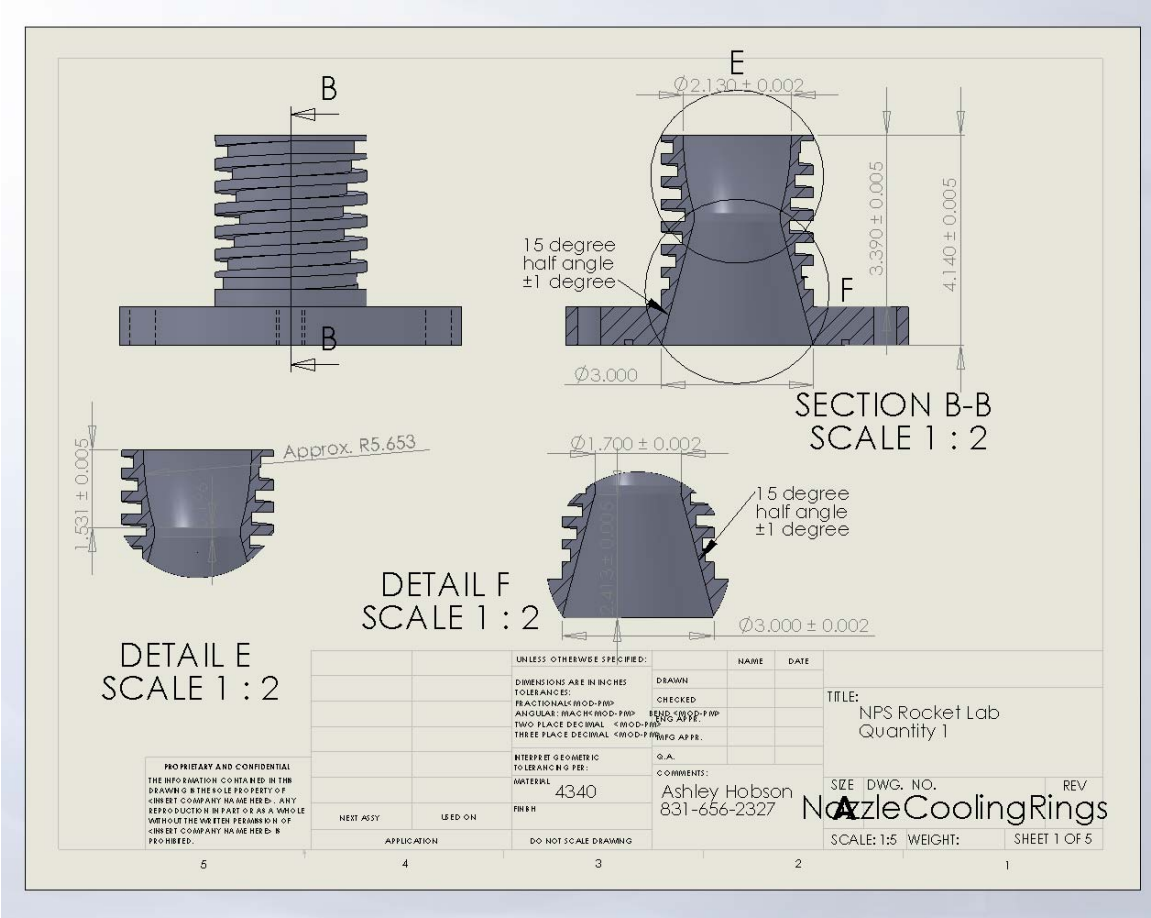

Figure 45. Cooling Nozzle – Inner Tube

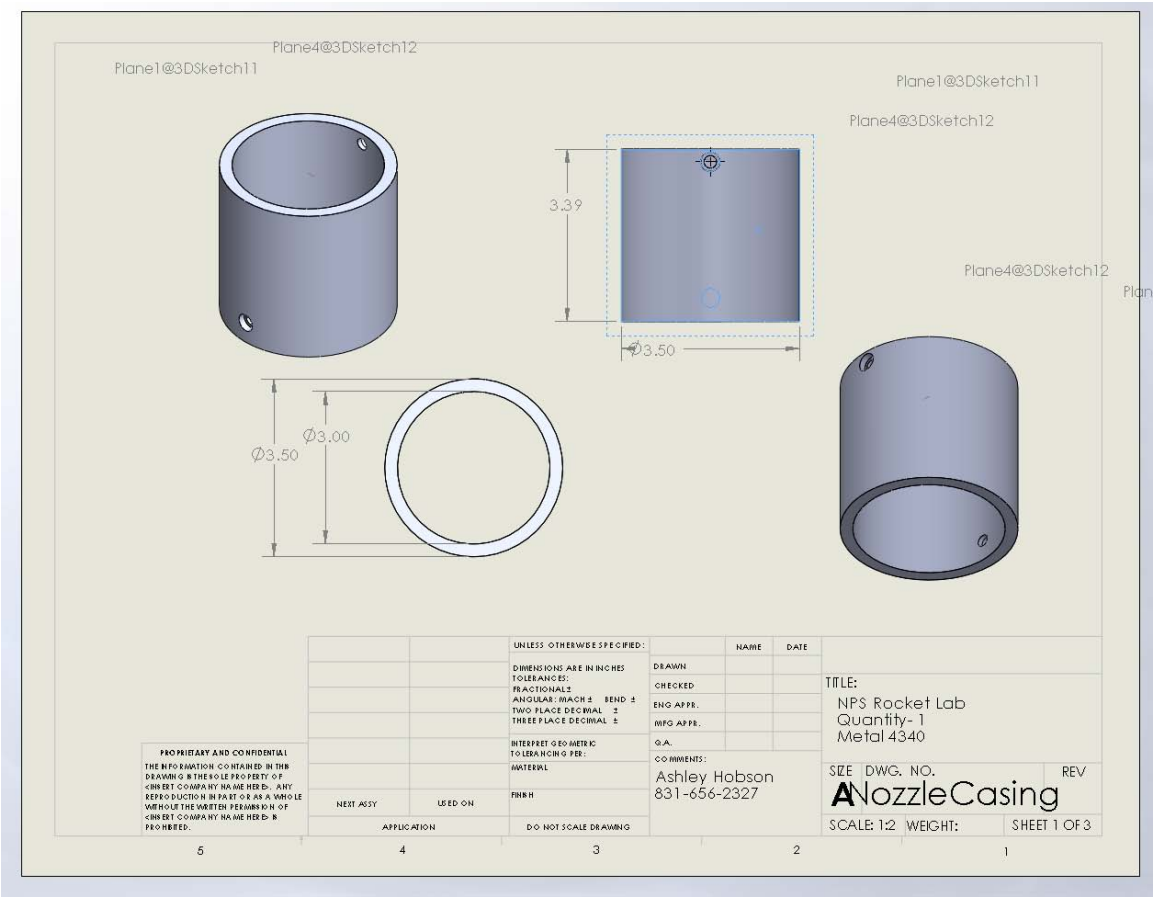

Figure 46. Cooling Nozzle – Outer Casing

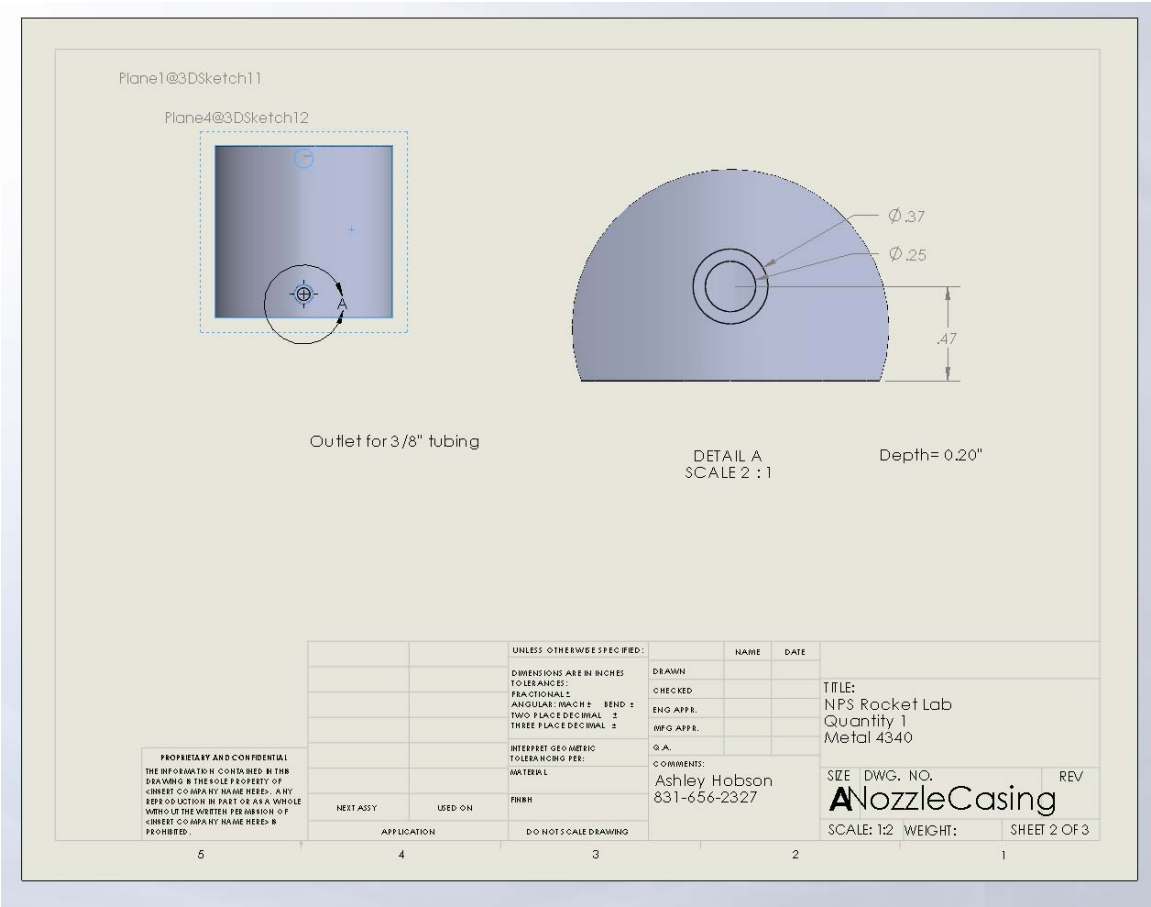

Figure 47. Cooling Nozzle – Water Outlet Detail

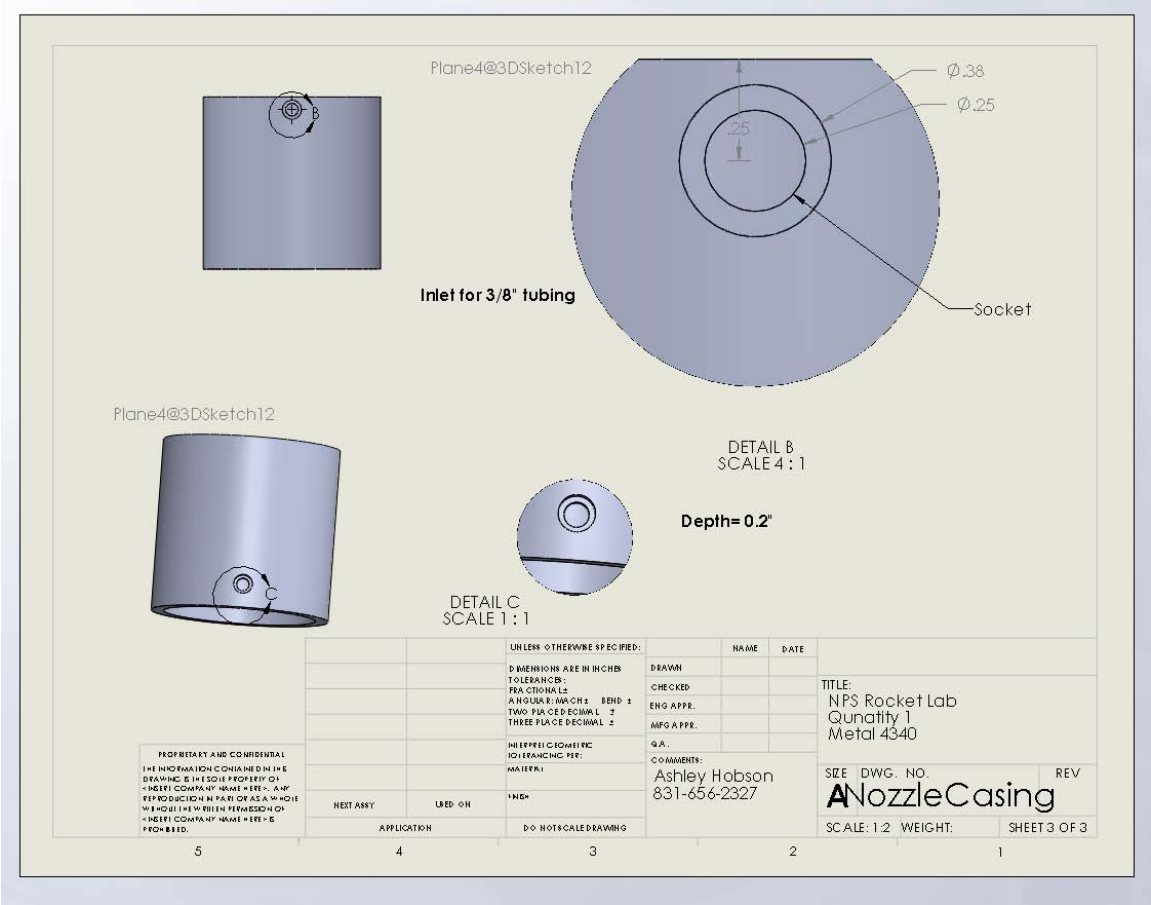

Figure 48. Cooling Nozzle – Water Inlet Detail

C. PRESSURE TRANSDUCER SPACERS

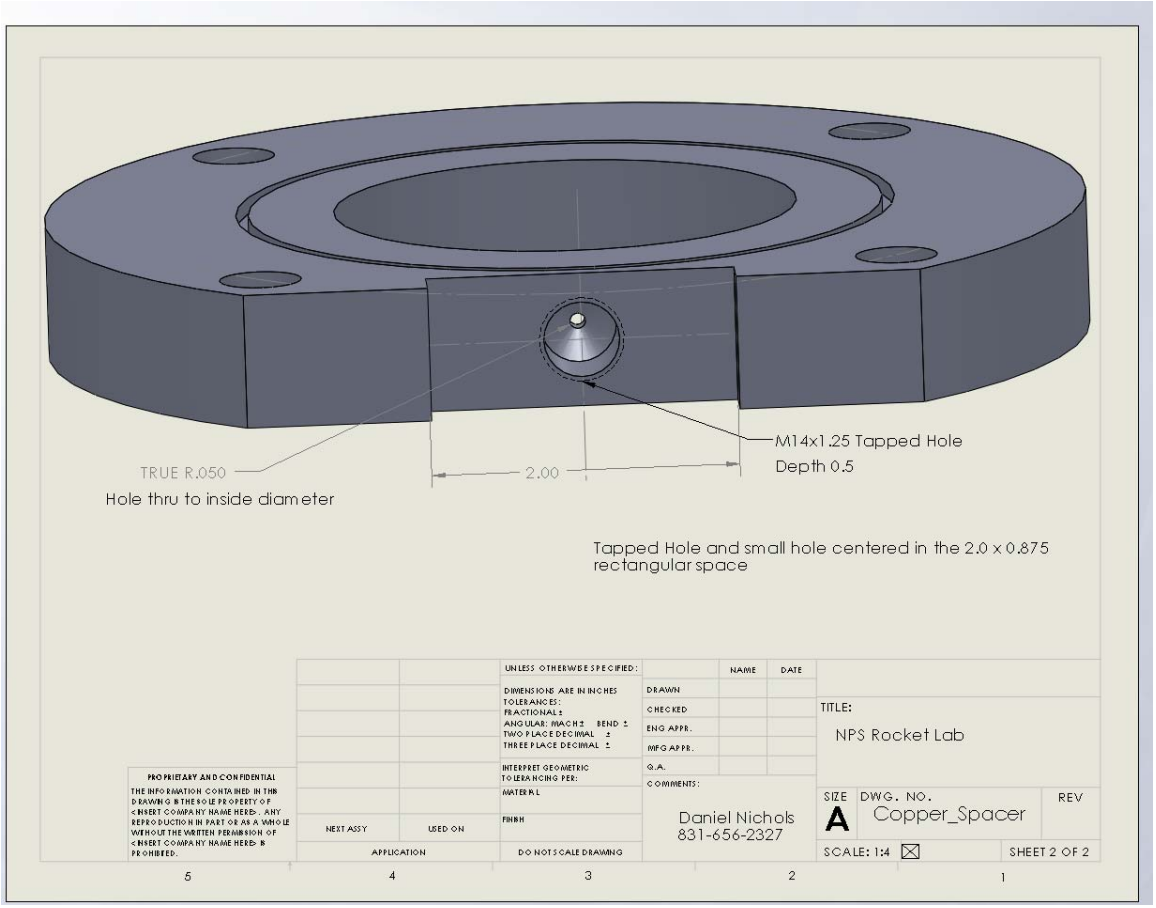

Figure 49. Pressure Transducer Spacer – Isometric View

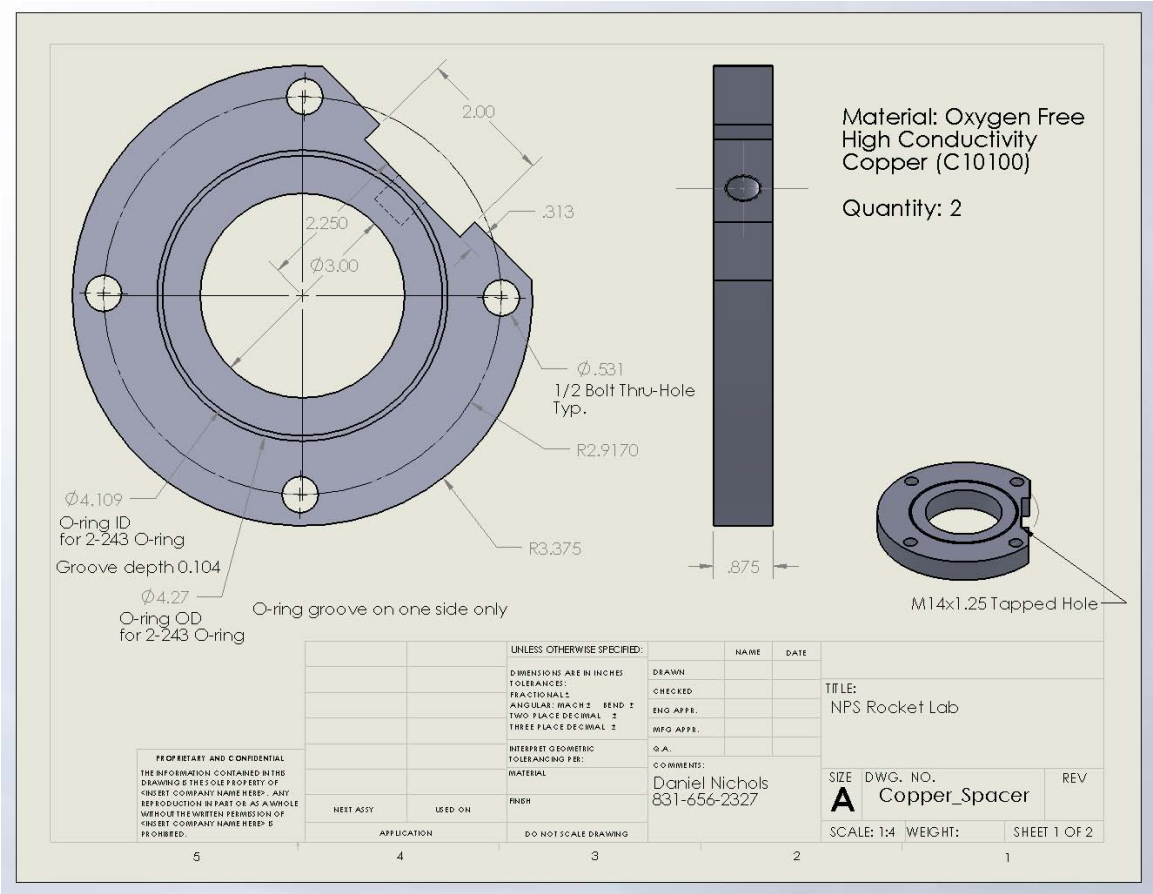

Figure 50. Pressure Transducer Spacer – Plan View

D. ADAPTER FLANGES

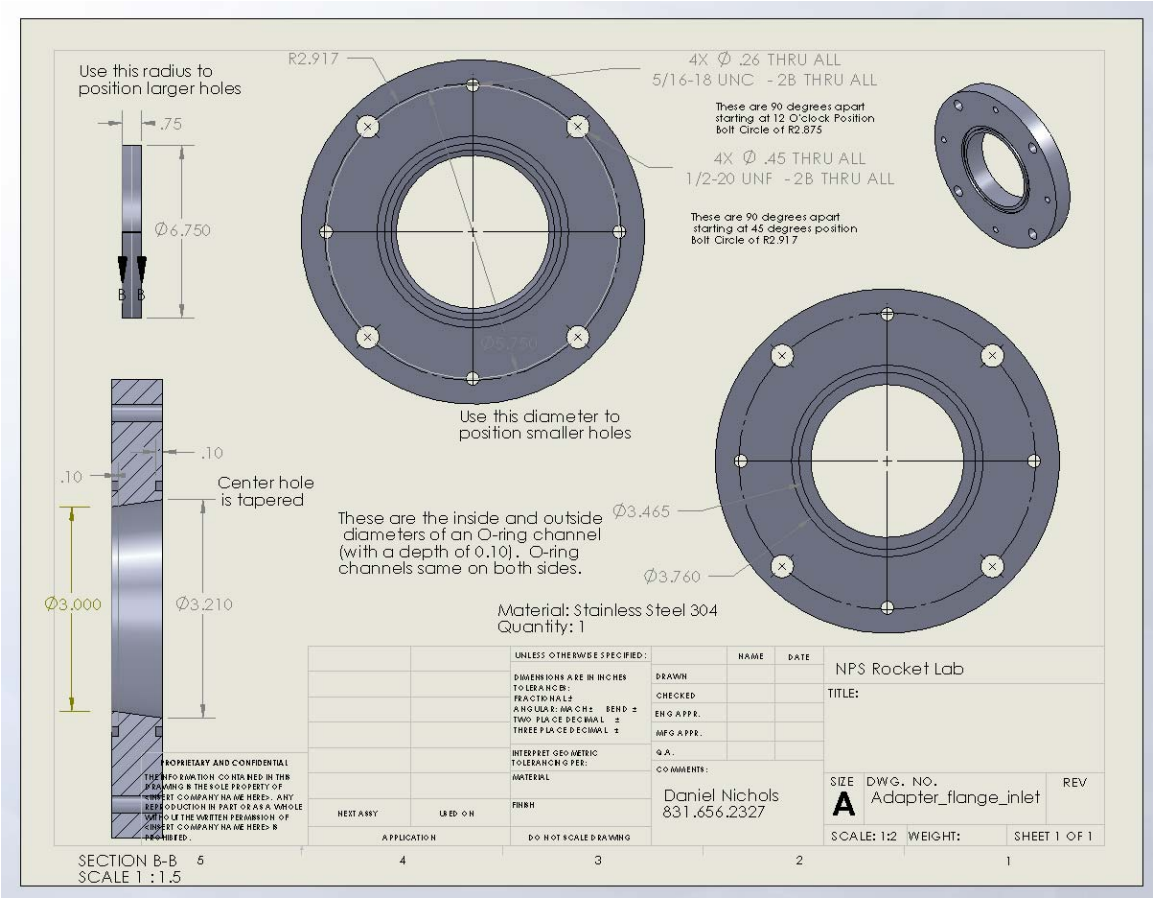

Figure 51. Adapter Flange – Inlet Side

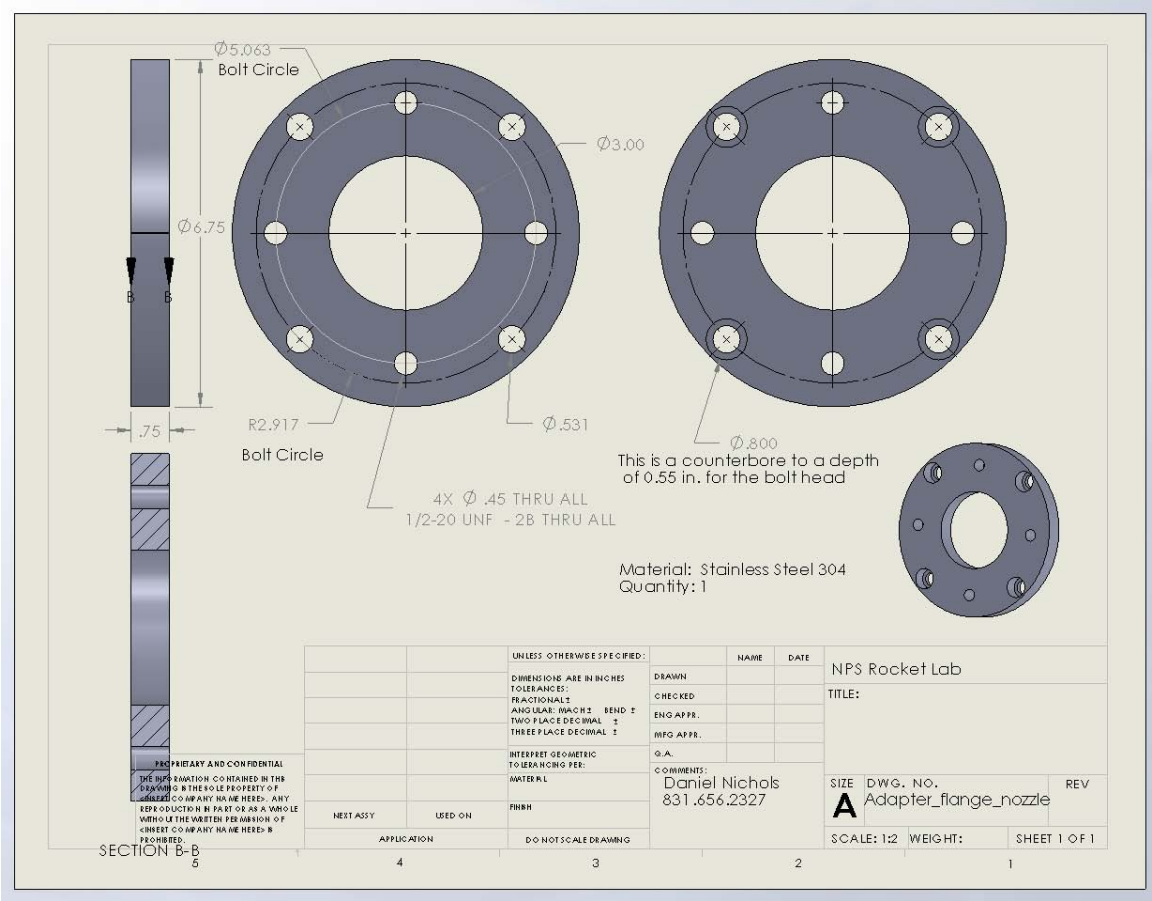

Figure 52. Adapter Flange – Nozzle Side

E. COMBUSTOR SUPPORT STAND

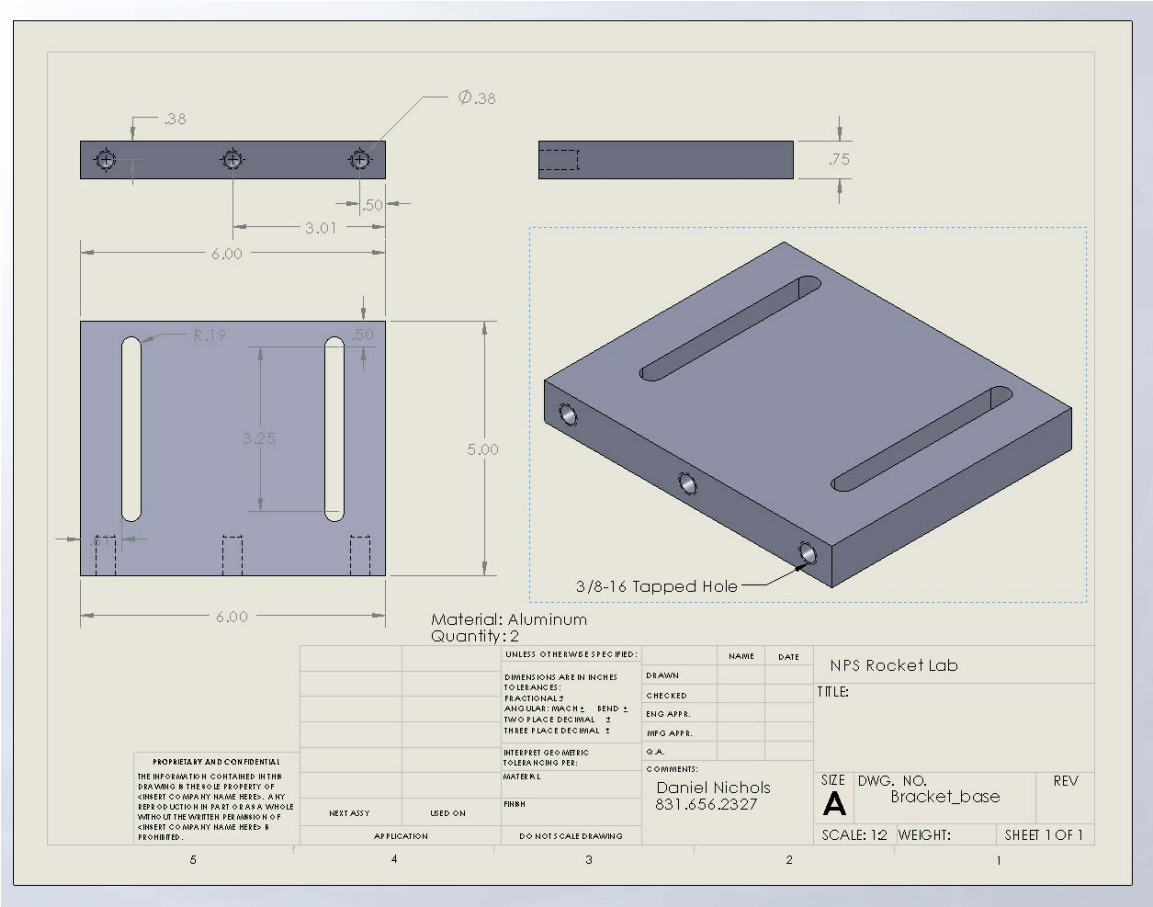

Figure 53. Combustor Support Stand – Base

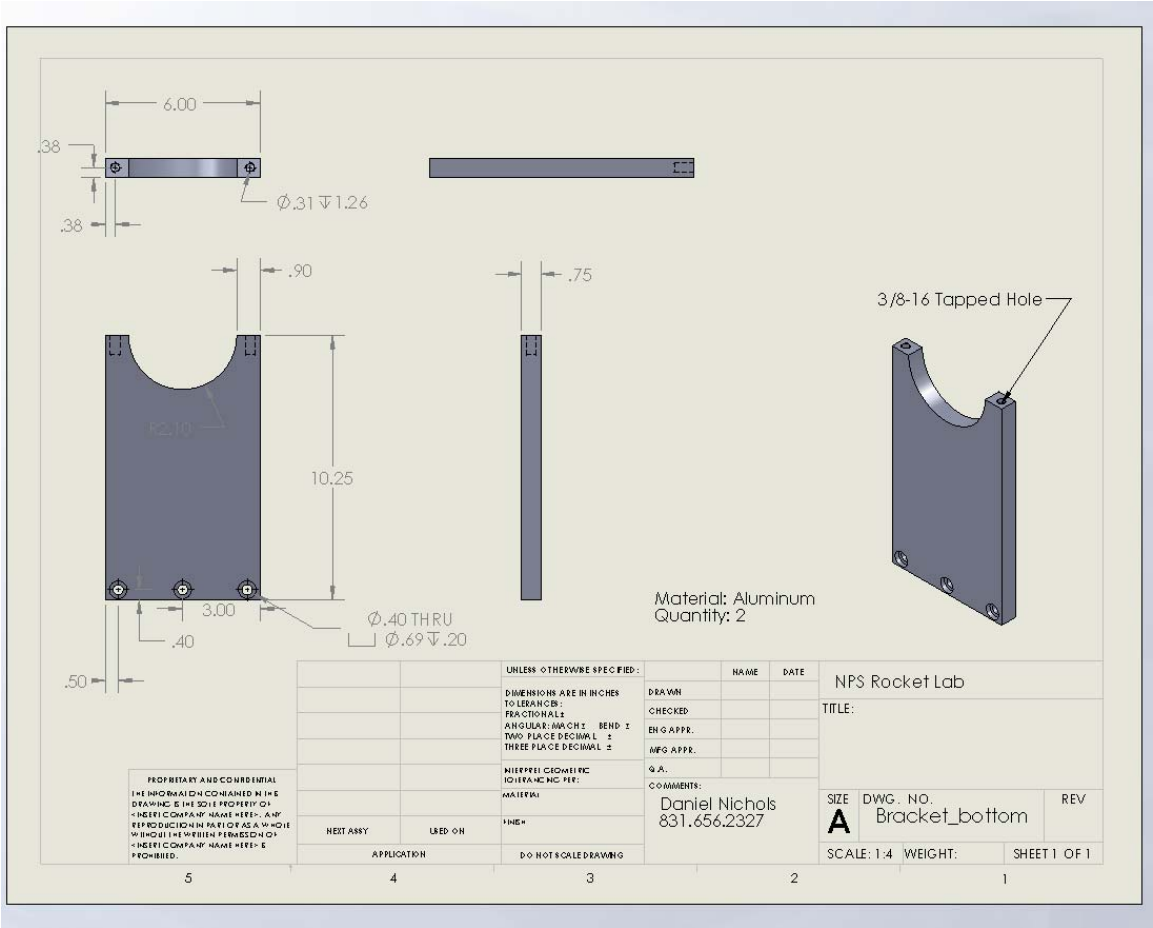

Figure 54. Combustor Support Stand – Bottom

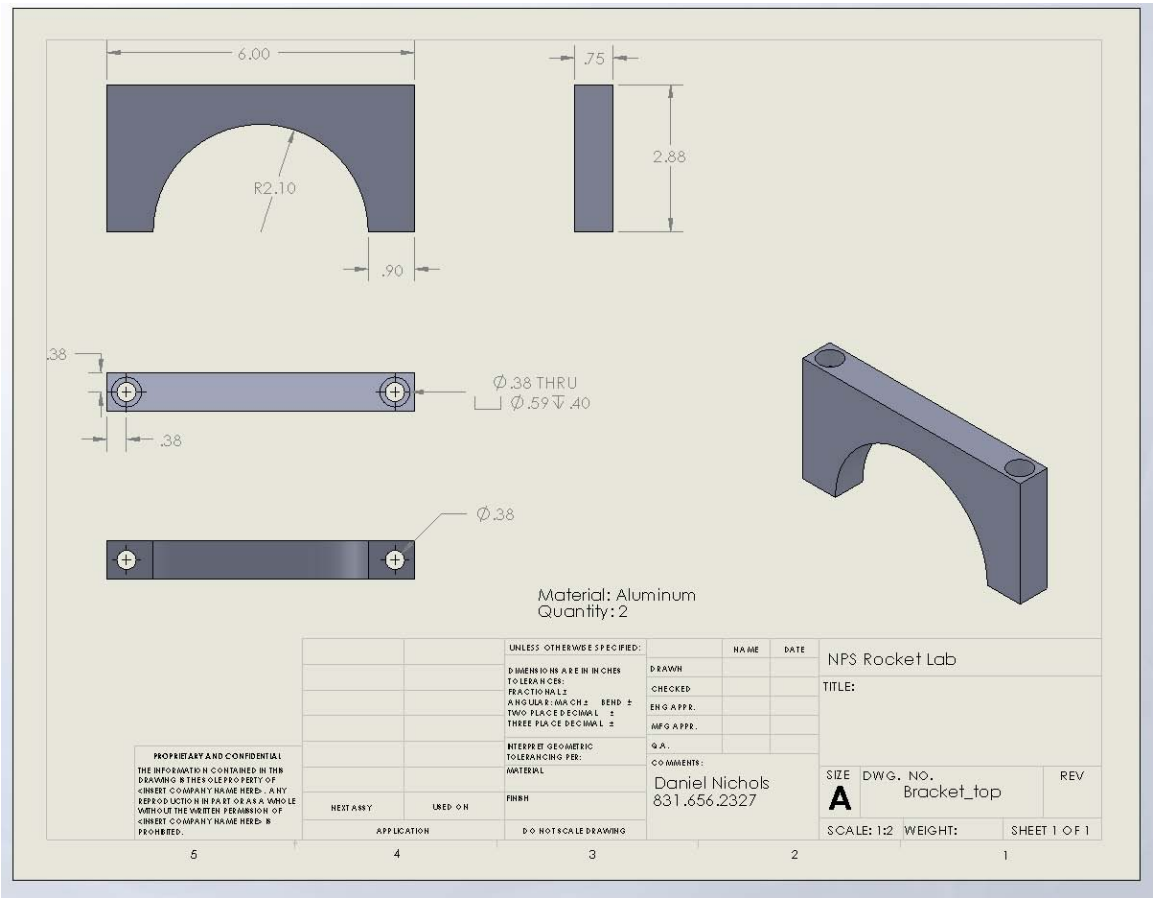

Figure 55. Combustor Support Stand – Top

THIS PAGE INTENTIONALLY LEFT BLANK

LIST OF REFERENCES

[1] J.A. Nichols, H.R. Wilkinson, and R. B. Morrison, "Intermittent detonation as a thrust-producing mechanism," *Jet Propulsion Journal of the American Rocket Society*, May 1957.

[2] P.G. Harris, S.M. Guzik, and R.A. Stowe, "Design methodology for a pulse detonation engine as a ramjet replacement," AIAA Paper 2004-3400, *Joint Propulsion Conference and Exhibit*, Fort Lauderdale, Florida, 11–14 July 2004.

[3] R. Friedman, "American rocket society," Vol. 24, p.349, November 1953.

[4] T. Bussing and G. Pappas, "Pulse detonation theory and concepts," *Developments in High-Speed Vehicle Propulsion Systems*, Progress in Aeronautics and Astronautics, Volume 165, AIAA, 1996.

[5] G. Ciccarelli, T. Ginsberg, J. Boccio, C. Economos, K. Sato, M. Kinoshita, "Detonation cell size measurements and predictions in hydrogen-air steam mixtures at elevated temperatures," *Combustion and Flame*, Volume 99, Issue 2, November 1994.

[6] W. T. Dvorak, *Performance Characterization of Swept Ramp Obstacle Fields in Pulse Detonation Applications*, M.S. Thesis, Naval Postgraduate School, Monterey, California, March 2010.

[7] K. K. Kuo, *Principles of combustion*, 2nd edition, John Wiley & Sons, Inc., 2005.

[8] T. Bussing and G. Pappas, "An introduction to pulse detonation engines," AIAA Paper 1994-0263, *32nd AIAA Aerospace Sciences Meeting and Exhibit*, Reno, Nevada, January 1994.

[9] A. J. Higgins, P. Pinard, A.C. Yoshinaka, and J.H.S. Lee, "Sensitization of fuel-air mixtures for deflagration-to-detonation transition," in G. Roy, S. Frolov, D. Netzer, and A. Borisov, *High-Speed Deflagration and Detonation: Fundamentals and Control*, pp. 45–49, ELEX-KM Publishers, 2001.

[10] P. D. Hutcheson, *Design, Modeling and Performance of a Split Path JP-10/Air Pulse Detonation Engine*, M.S. Thesis, Naval Postgraduate School, Monterey, California, December 2006.

[11] N. C. Hawkes, *Characterization of Transient Plasma Ignition Kernel Growth for Varying Inlet Condition*, M.S. Thesis, Naval Postgraduate School, Monterey, California, December 2009.

[12] Kistler Instrument Corporation, *Type 603B1 Miniature, High Frequency, Charge Output Pressure Sensor Data Sheet*, 2003.

INITIAL DISTRIBUTION LIST

1. Defense Technical Information Center
   Ft. Belvoir, Virginia

2. Dudley Knox Library
   Naval Postgraduate School
   Monterey, California

3. Professor Christopher Brophy
   Naval Postgraduate School
   Monterey, California

4. Professor Anthony Gannon
   Naval Postgraduate School
   Monterey, California

5. LCDR Daniel Nichols
   Naval Postgraduate School
   Monterey, California

6. Professor Knox Millsaps
   Chairman, Mechanical and Aerospace Engineering
   Naval Postgraduate School
   Monterey, California